VII

Wavelet Bases

One can construct wavelets ψ such that the dilated and translated family

$$\left\{ \psi_{j,n}(t) = \frac{1}{\sqrt{2^j}} \psi\left(\frac{t - 2^j n}{2^j} \right) \right\}_{(j,n) \in \mathbb{Z}^2}$$

is an orthonormal basis of $\mathbf{L^2}(\mathbb{R})$. Behind this simple statement lie very different point of views which open a fruitful exchange between harmonic analysis and discrete signal processing.

Orthogonal wavelets dilated by 2^j carry signal variations at the resolution 2^{-j}. The construction of these bases can thus be related to multiresolution signal approximations. Following this link leads us to an unexpected equivalence between wavelet bases and conjugate mirror filters used in discrete multirate filter banks. These filter banks implement a fast orthogonal wavelet transform that requires only $O(N)$ operations for signals of size N. The design of conjugate mirror filters also gives new classes of wavelet orthogonal bases including regular wavelets of compact support. In several dimensions, wavelet bases of $\mathbf{L^2}(\mathbb{R}^d)$ are constructed with separable products of functions of one variable. Wavelet bases are also adapted to bounded domains and surfaces with lifting algorithms.

7.1 Orthogonal Wavelet Bases

Our search for orthogonal wavelets begins with multiresolution approximations. For $f \in \mathbf{L^2}(\mathbb{R})$, the partial sum of wavelet coefficients $\sum_{n=-\infty}^{+\infty} \langle f, \psi_{j,n} \rangle \psi_{j,n}$ can indeed be interpreted as the difference between two approximations of f at the resolutions 2^{-j+1} and 2^{-j}. Multiresolution approximations compute the approximation of signals at various resolutions with orthogonal projections on different spaces $\{\mathbf{V}_j\}_{j \in \mathbb{Z}}$. Section 7.1.3 proves that multiresolution approximations are entirely characterized by a particular discrete filter that governs the loss of information across resolutions. These discrete filters provide a simple procedure for designing and synthesizing orthogonal wavelet bases.

7.1.1 Multiresolution Approximations

Adapting the signal resolution allows one to process only the relevant details for a particular task. In computer vision, Burt and Adelson [125] introduced a multiresolution pyramid that can be used to process a low-resolution image first and then selectively increase the resolution when necessary. This section formalizes multiresolution approximations, which set the ground for the construction of orthogonal wavelets.

The approximation of a function f at a resolution 2^{-j} is specified by a discrete grid of samples that provides local averages of f over neighborhoods of size proportional to 2^j. A multiresolution approximation is thus composed of embedded grids of approximation. More formally, the approximation of a function at a resolution 2^{-j} is defined as an orthogonal projection on a space

$\mathbf{V}_j \subset \mathbf{L^2}(\mathbb{R})$. The space $\mathbf{V}_j$ regroups all possible approximations at the resolution 2^{-j}. The orthogonal projection of f is the function $f_j \in \mathbf{V}_j$ that minimizes $\|f - f_j\|$. The following definition introduced by Mallat [361] and Meyer [43] specifies the mathematical properties of multiresolution spaces. To avoid confusion, let us emphasize that a scale parameter 2^j is the inverse of the resolution 2^{-j}.

Definition 7.1 (Multiresolutions). *A sequence $\{\mathbf{V}_j\}_{j\in\mathbb{Z}}$ of closed subspaces of $\mathbf{L^2}(\mathbb{R})$ is a multiresolution approximation if the following 6 properties are satisfied:*

$$\forall (j,k) \in \mathbb{Z}^2 \quad , \quad f(t) \in \mathbf{V}_j \;\Leftrightarrow\; f(t - 2^j k) \in \mathbf{V}_j \;, \tag{7.1}$$

$$\forall j \in \mathbb{Z} \quad , \quad \mathbf{V}_{j+1} \subset \mathbf{V}_j \;, \tag{7.2}$$

$$\forall j \in \mathbb{Z} \quad , \quad f(t) \in \mathbf{V}_j \;\Leftrightarrow\; f\left(\frac{t}{2}\right) \in \mathbf{V}_{j+1} \;, \tag{7.3}$$

$$\lim_{j\to+\infty} \mathbf{V}_j = \bigcap_{j=-\infty}^{+\infty} \mathbf{V}_j = \{0\} \;, \tag{7.4}$$

$$\lim_{j\to-\infty} \mathbf{V}_j = \text{Closure}\left(\bigcup_{j=-\infty}^{+\infty} \mathbf{V}_j\right) = \mathbf{L^2}(\mathbb{R}) \;. \tag{7.5}$$

There exists θ such that $\{\theta(t-n)\}_{n\in\mathbb{Z}}$ is a Riesz basis of $\mathbf{V}_0$.

Let us give an intuitive explanation of these mathematical properties. Property (7.1) means that $\mathbf{V}_j$ is invariant by any translation proportional to the scale 2^j. As we shall see later, this space can be assimilated to a uniform grid with intervals 2^j, which characterizes the signal approximation at the resolution 2^{-j}. The inclusion (7.2) is a causality property which proves that an approximation at a resolution 2^{-j} contains all the necessary information to compute an approximation at a coarser resolution 2^{-j-1}. Dilating functions in $\mathbf{V}_j$ by 2 enlarges the details by 2 and (7.3) guarantees that it defines an approximation at a coarser resolution 2^{-j-1}. When the resolution 2^{-j} goes to 0 (7.4) implies that we lose all the details of f and

$$\lim_{j\to+\infty} \|P_{\mathbf{V}_j} f\| = 0. \tag{7.6}$$

On the other hand, when the resolution 2^{-j} goes $+\infty$, property (7.5) imposes that the signal approximation converges to the original signal:

$$\lim_{j\to-\infty} \|f - P_{\mathbf{V}_j} f\| = 0. \tag{7.7}$$

When the resolution 2^{-j} increases, the decay rate of the approximation error $\|f - P_{\mathbf{V}_j} f\|$ depends on the regularity of f. Section 9.1.3 relates this error to the uniform Lipschitz regularity of f.

The existence of a Riesz basis $\{\theta(t-n)\}_{n\in\mathbb{Z}}$ of $\mathbf{V}_0$ provides a discretization theorem as explained in Section 3.1.3. The function θ can be interpreted as a unit resolution cell; Section 5.1.1 gives the definition of a Riesz basis. It is a family of linearly independent functions such that there exist $B \geqslant A > 0$ which satisfy

$$\forall f \in \mathbf{V}_0 \quad , \quad A\,\|f\|^2 \leqslant \sum_{n=-\infty}^{+\infty} |\langle f(t), \theta(t-n)\rangle|^2 \leqslant B\,\|f\|^2 \;. \tag{7.8}$$

This energy equivalence guarantees that signal expansions over $\{\theta(t-n)\}_{n\in\mathbb{Z}}$ are numerically stable. One verify that the family $\{2^{-j/2}\theta(2^{-j}t-n)\}_{n\in\mathbb{Z}}$ is a Riesz basis of $\mathbf{V}_j$ with the same Riesz bounds A and B at all scales 2^j. Theorem 3.4 proves that $\{\theta(t-n)\}_{n\in\mathbb{Z}}$ is a Riesz basis if and only if

$$\forall \omega \in [-\pi,\pi] \quad , \quad A \leqslant \sum_{k=-\infty}^{+\infty} |\hat{\theta}(\omega + 2k\pi)|^2 \leqslant B. \tag{7.9}$$

Example 7.1. Piecewise constant approximations *A simple multiresolution approximation is composed of piecewise constant functions. The space $\mathbf{V}_j$ is the set of all $g \in \mathbf{L^2}(\mathbb{R})$ such that $g(t)$ is constant for $t \in [n2^j, (n+1)2^j)$ and $n \in \mathbb{Z}$. The approximation at a resolution 2^{-j} of f is the closest piecewise constant function on intervals of size 2^j. The resolution cell can be chosen to be the box window $\theta = \mathbf{1}_{[0,1)}$. Clearly $\mathbf{V}_j \subset \mathbf{V}_{j-1}$ since functions constant on intervals of size 2^j are also constant on intervals of size 2^{j-1}. The verification of the other multiresolution properties is left to the reader. It is often desirable to construct approximations that are smooth functions, in which case piecewise constant functions are not appropriate.*

Example 7.2. Shannon approximations *Frequency band-limited functions also yield multiresolution approximations. The space $\mathbf{V}_j$ is defined as the set of functions whose Fourier transform has a support included in $[-2^{-j}\pi, 2^{-j}\pi]$. Theorem 3.5 provides an orthonormal basis $\{\theta(t-n)\}_{n\in\mathbb{Z}}$ of $\mathbf{V}_0$ defined by*

$$\theta(t) = \frac{\sin \pi t}{\pi t}. \tag{7.10}$$

All other properties of multiresolution approximation are easily verified.

The approximation at the resolution 2^{-j} of $f \in \mathbf{L^2}(\mathbb{R})$ is the function $P_{\mathbf{V}_j} f \in \mathbf{V}_j$ that minimizes $\|P_{\mathbf{V}_j} f - f\|$. It is proved in (3.12) that its Fourier transform is obtained with a frequency filtering:

$$\widehat{P_{\mathbf{V}_j} f}(\omega) = \hat{f}(\omega)\, \mathbf{1}_{[-2^{-j}\pi, 2^{-j}\pi]}(\omega).$$

This Fourier transform is generally discontinuous at $\pm 2^{-j}\pi$, in which case $|P_{\mathbf{V}_j} f(t)|$ decays like $|t|^{-1}$, for large $|t|$, even though f might have a compact support.

Example 7.3. Spline approximations *Polynomial spline approximations construct smooth approximations with fast asymptotic decay. The space $\mathbf{V}_j$ of splines of degree $m \geqslant 0$ is the set of functions that are $m-1$ times continuously differentiable and equal to a polynomial of degree m on any interval $[n2^j, (n+1)2^j]$, for $n \in \mathbb{Z}$. When $m = 0$, it is a piecewise constant multiresolution approximation. When $m = 1$, functions in $\mathbf{V}_j$ are piecewise linear and continuous.*

A Riesz basis of polynomial splines is constructed with box splines. A box spline θ of degree m is computed by convolving the box window $\mathbf{1}_{[0,1]}$ with itself $m+1$ times and centering at 0 or $1/2$. Its Fourier transform is

$$\hat{\theta}(\omega) = \left(\frac{\sin(\omega/2)}{\omega/2}\right)^{m+1} \exp\left(\frac{-i\varepsilon\omega}{2}\right). \tag{7.11}$$

If m is even then $\varepsilon = 1$ and θ has a support centered at $t = 1/2$. If m is odd then $\varepsilon = 0$ and $\theta(t)$ is symmetric about $t = 0$. Figure 7.1 displays a cubic box spline $m = 3$ and its Fourier transform. For all $m \geqslant 0$, one can prove that $\{\theta(t-n)\}_{n\in\mathbb{Z}}$ is a Riesz basis of $\mathbf{V}_0$ by verifying the condition (7.9). This is done with a closed form expression for the series (7.19).

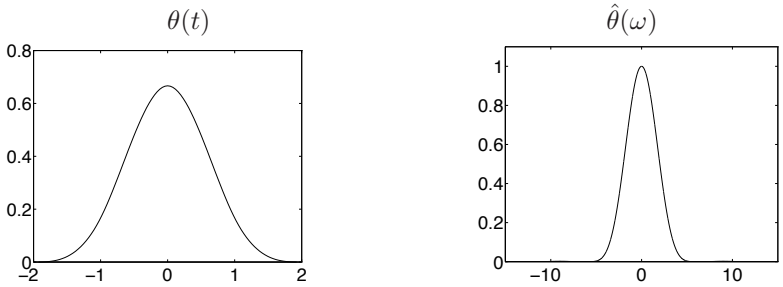

Figure 7.1: Cubic box spline θ and its Fourier transform $\hat{\theta}$.

7.1.2 Scaling Function

The approximation of f at the resolution 2^{-j} is defined as the orthogonal projection $P_{\mathbf{V}_j} f$ on $\mathbf{V}_j$. To compute this projection, we must find an orthonormal basis of $\mathbf{V}_j$. The following theorem

orthogonalizes the Riesz basis $\{\theta(t-n)\}_{n\in\mathbb{Z}}$ and constructs an orthogonal basis of each space $\mathbf{V}_j$ by dilating and translating a single function ϕ called a *scaling function*. To avoid confusing the resolution 2^{-j} and the scale 2^j, in the rest of the chapter the notion of resolution is dropped and $P_{\mathbf{V}_j} f$ is called an approximation at the scale 2^j.

Theorem 7.1. *Let $\{\mathbf{V}_j\}_{j\in\mathbb{Z}}$ be a multiresolution approximation and ϕ be the scaling function whose Fourier transform is*

$$\hat{\phi}(\omega) = \frac{\hat{\theta}(\omega)}{\left(\sum_{k=-\infty}^{+\infty} |\hat{\theta}(\omega+2k\pi)|^2\right)^{1/2}}. \tag{7.12}$$

Let us denote

$$\phi_{j,n}(t) = \frac{1}{\sqrt{2^j}}\,\phi\left(\frac{t-n}{2^j}\right).$$

The family $\{\phi_{j,n}\}_{n\in\mathbb{Z}}$ is an orthonormal basis of $\mathbf{V}_j$ for all $j\in\mathbb{Z}$.

Proof. To construct an orthonormal basis, we look for a function $\phi\in\mathbf{V}_0$. It can thus be expanded in the basis $\{\theta(t-n)\}_{n\in\mathbb{Z}}$:

$$\phi(t) = \sum_{n=-\infty}^{+\infty} a[n]\,\theta(t-n),$$

which implies that

$$\hat{\phi}(\omega) = \hat{a}(\omega)\,\hat{\theta}(\omega),$$

where $\hat{a}$ is a 2π periodic Fourier series of finite energy. To compute $\hat{a}$ we express the orthogonality of $\{\phi(t-n)\}_{n\in\mathbb{Z}}$ in the Fourier domain. Let $\bar{\phi}(t)=\phi^*(-t)$. For any $(n,p)\in\mathbb{Z}^2$,

$$\begin{aligned}\langle \phi(t-n), \phi(t-p)\rangle &= \int_{-\infty}^{+\infty} \phi(t-n)\,\phi^*(t-p)\,dt \\ &= \phi\star\bar{\phi}(p-n)\ . \end{aligned}\tag{7.13}$$

Hence $\{\phi(t-n)\}_{n\in\mathbb{Z}}$ is orthonormal if and only if $\phi\star\bar{\phi}(n)=\delta[n]$. Computing the Fourier transform of this equality yields

$$\sum_{k=-\infty}^{+\infty} |\hat{\phi}(\omega+2k\pi)|^2 = 1. \tag{7.14}$$

Indeed, the Fourier transform of $\phi\star\bar{\phi}(t)$ is $|\hat{\phi}(\omega)|^2$, and we we proved in (3.3) that sampling a function periodizes its Fourier transform. The property (7.14) is verified if we choose

$$\hat{a}(\omega) = \left(\sum_{k=-\infty}^{+\infty} |\hat{\theta}(\omega+2k\pi)|^2\right)^{-1/2}.$$

We saw in (7.9) that the denominator has a strictly positive lower bound, so $\hat{a}$ is a 2π periodic function of finite energy. ■ ■

Approximation The orthogonal projection of f over $\mathbf{V}_j$ is obtained with an expansion in the scaling orthogonal basis

$$P_{\mathbf{V}_j} f = \sum_{n=-\infty}^{+\infty} \langle f, \phi_{j,n}\rangle\,\phi_{j,n}. \tag{7.15}$$

The inner products

$$a_j[n] = \langle f, \phi_{j,n}\rangle \tag{7.16}$$

provide a discrete approximation at the scale 2^j. We can rewrite them as a convolution product:

$$a_j[n] = \int_{-\infty}^{+\infty} f(t)\,\frac{1}{\sqrt{2^j}}\,\phi\left(\frac{t-2^j n}{2^j}\right)dt = f\star\bar{\phi}_j(2^j n), \tag{7.17}$$

with $\bar{\phi}_j(t) = \sqrt{2^{-j}}\phi(2^{-j}t)$. The energy of the Fourier transform $\hat{\phi}$ is typically concentrated in $[-\pi,\pi]$, as illustrated by Figure 7.2. As a consequence, the Fourier transform $\sqrt{2^j}\hat{\phi}^*(2^j\omega)$ of $\bar{\phi}_j(t)$

is mostly non-negligible in $[-2^{-j}\pi, 2^{-j}\pi]$. The discrete approximation $a_j[n]$ is therefore a low-pass filtering of f sampled at intervals 2^j. Figure 7.3 gives a discrete multiresolution approximation at scales $2^{-9} \leqslant 2^j \leqslant 2^{-4}$.

Example 7.4. *For piecewise constant approximations and Shannon multiresolution approximations we have constructed Riesz bases $\{\theta(t-n)\}_{n\in\mathbb{Z}}$ which are orthonormal bases, hence $\phi = \theta$.*

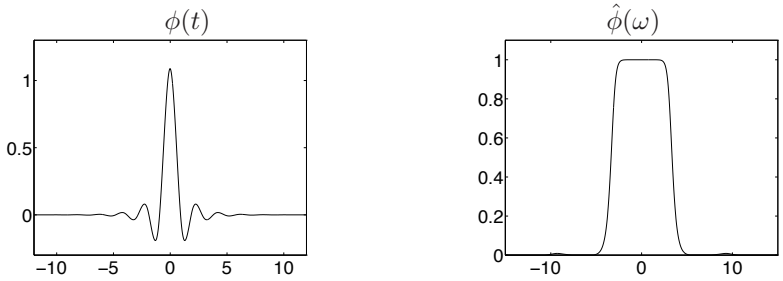

Figure 7.2: Cubic spline scaling function ϕ and its Fourier transform $\hat{\phi}$ computed with (7.18).

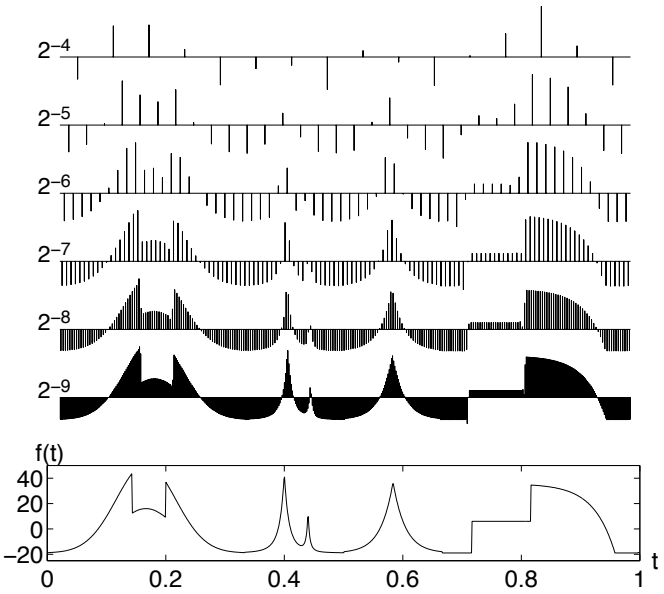

Figure 7.3: Discrete multiresolution approximations $a_j[n]$ at scales 2^j, computed with cubic splines.

Example 7.5. *Spline multiresolution approximations admit a Riesz basis constructed with a box spline θ of degree m, whose Fourier transform is given by (7.11). Inserting this expression in (7.12) yields*

$$\hat{\phi}(\omega) = \frac{\exp\left(-i\varepsilon\omega/2\right)}{\omega^{m+1}\sqrt{S_{2m+2}(\omega)}}, \tag{7.18}$$

with

$$S_n(\omega) = \sum_{k=-\infty}^{+\infty} \frac{1}{(\omega + 2k\pi)^n}, \tag{7.19}$$

and $\varepsilon = 1$ if m is even or $\varepsilon = 0$ if m is odd. A closed form expression of $S_{2m+2}(\omega)$ is obtained by computing the derivative of order $2m$ of the identity

$$S_2(2\omega) = \sum_{k=-\infty}^{+\infty} \frac{1}{(2\omega + 2k\pi)^2} = \frac{1}{4\sin^2\omega}.$$

For linear splines $m = 1$ and

$$S_4(2\omega) = \frac{1 + 2\cos^2 \omega}{48 \sin^4 \omega}, \tag{7.20}$$

which yields

$$\hat{\phi}(\omega) = \frac{4\sqrt{3}\sin^2(\omega/2)}{\omega^2 \sqrt{1 + 2\cos^2(\omega/2)}}. \tag{7.21}$$

The cubic spline scaling function corresponds to $m = 3$ and $\hat{\phi}(\omega)$ is calculated with (7.18) by inserting

$$\begin{aligned} S_8(2\omega) &= \frac{5 + 30\cos^2 \omega + 30\sin^2 \omega \, \cos^2 \omega}{105\, 2^8 \, \sin^8 \omega} \\ &\quad + \frac{70\cos^4 \omega + 2\sin^4 \omega \, \cos^2 \omega + 2/3 \, \sin^6 \omega}{105\, 2^8 \, \sin^8 \omega}. \end{aligned} \tag{7.22}$$

This cubic spline scaling function ϕ and its Fourier transform are displayed in Figure 7.2. It has an infinite support but decays exponentially.

7.1.3 Conjugate Mirror Filters

A multiresolution approximation is entirely characterized by the scaling function ϕ that generates an orthogonal basis of each space $\mathbf{V}_j$. We study the properties of ϕ which guarantee that the spaces $\mathbf{V}_j$ satisfy all conditions of a multiresolution approximation. It is proved that any scaling function is specified by a discrete filter called a *conjugate mirror filter*.

Scaling Equation The multiresolution causality property (7.2) imposes that $\mathbf{V}_j \subset \mathbf{V}_{j-1}$. In particular $2^{-1/2}\phi(t/2) \in \mathbf{V}_1 \subset \mathbf{V}_0$. Since $\{\phi(t-n)\}_{n\in\mathbb{Z}}$ is an orthonormal basis of $\mathbf{V}_0$, we can decompose

$$\frac{1}{\sqrt{2}}\,\phi\Big(\frac{t}{2}\Big) = \sum_{n=-\infty}^{+\infty} h[n]\,\phi(t-n), \tag{7.23}$$

with

$$h[n] = \left\langle \frac{1}{\sqrt{2}}\phi\left(\frac{t}{2}\right), \phi(t-n) \right\rangle. \tag{7.24}$$

This scaling equation relates a dilation of ϕ by 2 to its integer translations. The sequence $h[n]$ will be interpreted as a discrete filter.

The Fourier transform of both sides of (7.23) yields

$$\hat{\phi}(2\omega) = \frac{1}{\sqrt{2}}\,\hat{h}(\omega)\,\hat{\phi}(\omega) \tag{7.25}$$

for $\hat{h}(\omega) = \sum_{n=-\infty}^{+\infty} h[n]\,\mathrm{e}^{-in\omega}$. It is thus tempting to express $\hat{\phi}(\omega)$ directly as a product of dilations of $\hat{h}(\omega)$. For any $p \geqslant 0$, (7.25) implies

$$\hat{\phi}(2^{-p+1}\omega) = \frac{1}{\sqrt{2}}\,\hat{h}(2^{-p}\omega)\,\hat{\phi}(2^{-p}\omega). \tag{7.26}$$

By substitution, we obtain

$$\hat{\phi}(\omega) = \left(\prod_{p=1}^{P} \frac{\hat{h}(2^{-p}\omega)}{\sqrt{2}}\right) \hat{\phi}(2^{-P}\omega). \tag{7.27}$$

If $\hat{\phi}(\omega)$ is continuous at $\omega = 0$ then $\lim_{P\to+\infty} \hat{\phi}(2^{-P}\omega) = \hat{\phi}(0)$ so

$$\hat{\phi}(\omega) = \prod_{p=1}^{+\infty} \frac{\hat{h}(2^{-p}\omega)}{\sqrt{2}}\,\hat{\phi}(0). \tag{7.28}$$

The following theorem [361, 43] gives necessary and then sufficient conditions on $\hat{h}(\omega)$ to guarantee that this infinite product is the Fourier transform of a scaling function.

Theorem 7.2 (Mallat, Meyer). *Let $\phi \in \mathbf{L^2}(\mathbb{R})$ be an integrable scaling function. The Fourier series of $h[n] = \langle 2^{-1/2}\phi(t/2), \phi(t-n)\rangle$ satisfies*

$$\forall \omega \in \mathbb{R} \quad , \quad |\hat{h}(\omega)|^2 + |\hat{h}(\omega+\pi)|^2 = 2, \tag{7.29}$$

and

$$\hat{h}(0) = \sqrt{2}. \tag{7.30}$$

Conversely, if $\hat{h}(\omega)$ is 2π periodic and continuously differentiable in a neighborhood of $\omega = 0$, if it satisfies (7.29) and (7.30) and if

$$\inf_{\omega \in [-\pi/2, \pi/2]} |\hat{h}(\omega)| > 0 \tag{7.31}$$

then

$$\hat{\phi}(\omega) = \prod_{p=1}^{+\infty} \frac{\hat{h}(2^{-p}\omega)}{\sqrt{2}} \tag{7.32}$$

is the Fourier transform of a scaling function $\phi \in \mathbf{L^2}(\mathbb{R})$.

Proof. This theorem is a central result whose proof is long and technical. It is divided in several parts.

• *Proof of the necessary condition (7.29)* The necessary condition is proved to be a consequence of the fact that $\{\phi(t-n)\}_{n\in\mathbb{Z}}$ is orthonormal. In the Fourier domain, (7.14) gives an equivalent condition:

$$\forall \omega \in \mathbb{R} \quad , \quad \sum_{k=-\infty}^{+\infty} |\hat{\phi}(\omega + 2k\pi)|^2 = 1. \tag{7.33}$$

Inserting $\hat{\phi}(\omega) = 2^{-1/2}\hat{h}(\omega/2)\,\hat{\phi}(\omega/2)$ yields

$$\sum_{k=-\infty}^{+\infty} |\hat{h}(\frac{\omega}{2} + k\pi)|^2\, |\hat{\phi}(\frac{\omega}{2} + k\pi)|^2 = 2.$$

Since $\hat{h}(\omega)$ is 2π periodic, separating the even and odd integer terms gives

$$|\hat{h}(\frac{\omega}{2})|^2 \sum_{p=-\infty}^{+\infty} \left|\hat{\phi}\left(\frac{\omega}{2} + 2p\pi\right)\right|^2 + \left|\hat{h}\left(\frac{\omega}{2} + \pi\right)\right|^2 \sum_{p=-\infty}^{+\infty} \left|\hat{\phi}\left(\frac{\omega}{2} + \pi + 2p\pi\right)\right|^2 = 2.$$

Inserting (7.33) for $\omega' = \omega/2$ and $\omega' = \omega/2 + \pi$ proves that

$$|\hat{h}(\omega')|^2 + |\hat{h}(\omega'+\pi)|^2 = 2.$$

• *Proof of the necessary condition (7.30)* We prove that $\hat{h}(0) = \sqrt{2}$ by showing that $\hat{\phi}(0) \neq 0$. Indeed we know that $\hat{\phi}(0) = 2^{-1/2}\,\hat{h}(0)\,\hat{\phi}(0)$. More precisely,we verify that $|\hat{\phi}(0)| = 1$ is a consequence of the completeness property (7.5) of multiresolution approximations.

The orthogonal projection of $f \in \mathbf{L^2}(\mathbb{R})$ on $\mathbf{V}_j$ is

$$P_{\mathbf{V}_j} f \;=\; \sum_{n=-\infty}^{+\infty} \langle f, \phi_{j,n}\rangle\, \phi_{j,n}. \tag{7.34}$$

Property (7.5) expressed in the time and Fourier domains with the Plancherel formula implies that

$$\lim_{j\to-\infty} \|f - P_{\mathbf{V}_j} f\|^2 = \lim_{j\to-\infty} 2\pi\, \|\hat{f} - \widehat{P_{\mathbf{V}_j} f}\|^2 = 0. \tag{7.35}$$

To compute the Fourier transform $\widehat{P_{\mathbf{V}_j} f}(\omega)$, we denote $\phi_j(t) = \sqrt{2^{-j}}\phi(2^{-j}t)$. Inserting the convolution expression (7.17) in (7.34) yields

$$P_{\mathbf{V}_j} f(t) = \sum_{n=-\infty}^{+\infty} f \star \bar{\phi}_j(2^j n)\, \phi_j(t - 2^j n) = \phi_j \star \sum_{n=-\infty}^{+\infty} f \star \bar{\phi}_j(2^j n)\, \delta(t - 2^j n).$$

The Fourier transform of $f \star \bar{\phi}_j(t)$ is $\sqrt{2^j}\hat{f}(\omega)\hat{\phi}^*(2^j\omega)$. A uniform sampling has a periodized Fourier transform calculated in (3.3), and hence

$$\widehat{P_{\mathbf{V}_j} f}(\omega) = \hat{\phi}(2^j\omega) \sum_{k=-\infty}^{+\infty} \hat{f}\left(\omega - \frac{2k\pi}{2^j}\right) \hat{\phi}^*\left(2^j\left[\omega - \frac{2k\pi}{2^j}\right]\right). \tag{7.36}$$

Let us choose $\hat{f} = \mathbf{1}_{[-\pi,\pi]}$. For $j < 0$ and $\omega \in [-\pi, \pi]$, (7.36) gives $\widehat{P_{\mathbf{V}_j} f}(\omega) = |\hat{\phi}(2^j\omega)|^2$. The mean-square convergence (7.35) implies that

$$\lim_{j \to -\infty} \int_{-\pi}^{\pi} \left|1 - |\hat{\phi}(2^j\omega)|^2\right|^2 d\omega = 0 \ .$$

Since ϕ is integrable, $\hat{\phi}(\omega)$ is continuous and hence $\lim_{j\to-\infty} |\hat{\phi}(2^j\omega)| = |\hat{\phi}(0)| = 1$.

We now prove that the function ϕ whose Fourier transform is given by (7.32) is a scaling function. This is divided in two intermediate results.

• *Proof that* $\{\phi(t-n)\}_{n\in\mathbb{Z}}$ *is orthonormal.* Observe first that the infinite product (7.32) converges and that $|\hat{\phi}(\omega)| \leqslant 1$ because (7.29) implies that $|\hat{h}(\omega)| \leqslant \sqrt{2}$. The Parseval formula gives

$$\langle \phi(t), \phi(t-n) \rangle = \int_{-\infty}^{+\infty} \phi(t)\, \phi^*(t-n)\, dt = \frac{1}{2\pi} \int_{-\infty}^{+\infty} |\hat{\phi}(\omega)|^2\, \mathrm{e}^{in\omega}\, d\omega.$$

Verifying that $\{\phi(t-n)\}_{n\in\mathbb{Z}}$ is orthonormal is thus equivalent to showing that

$$\int_{-\infty}^{+\infty} |\hat{\phi}(\omega)|^2\, \mathrm{e}^{in\omega}\, d\omega = 2\pi\, \delta[n].$$

This result is obtained by considering the functions

$$\hat{\phi}_k(\omega) = \prod_{p=1}^{k} \frac{\hat{h}(2^{-p}\omega)}{\sqrt{2}}\, \mathbf{1}_{[-2^k\pi, 2^k\pi]}(\omega).$$

and computing the limit, as k increases to $+\infty$, of the integrals

$$I_k[n] = \int_{-\infty}^{+\infty} |\hat{\phi}_k(\omega)|^2\, \mathrm{e}^{in\omega}\, d\omega = \int_{-2^k\pi}^{2^k\pi} \prod_{p=1}^{k} \frac{|\hat{h}(2^{-p}\omega)|^2}{2}\, \mathrm{e}^{in\omega}\, d\omega.$$

First, let us show that $I_k[n] = 2\pi\delta[n]$ for all $k \geqslant 1$. To do this, we divide $I_k[n]$ into two integrals:

$$I_k[n] = \int_{-2^k\pi}^{0} \prod_{p=1}^{k} \frac{|\hat{h}(2^{-p}\omega)|^2}{2}\, \mathrm{e}^{in\omega}\, d\omega + \int_{0}^{2^k\pi} \prod_{p=1}^{k} \frac{|\hat{h}(2^{-p}\omega)|^2}{2}\, \mathrm{e}^{in\omega}\, d\omega.$$

Let us make the change of variable $\omega' = \omega + 2^k\pi$ in the first integral. Since $\hat{h}(\omega)$ is 2π periodic, when $p < k$ then $|\hat{h}(2^{-p}[\omega' - 2^k\pi])|^2 = |\hat{h}(2^{-p}\omega')|^2$. When $k = p$ the hypothesis (7.29) implies that

$$|\hat{h}(2^{-k}[\omega' - 2^k\pi])|^2 + |\hat{h}(2^{-k}\omega')|^2 = 2.$$

For $k > 1$, the two integrals of $I_k[n]$ become

$$I_k[n] = \int_{0}^{2^k\pi} \prod_{p=1}^{k-1} \frac{|\hat{h}(2^{-p}\omega)|^2}{2}\, \mathrm{e}^{in\omega}\, d\omega\,. \tag{7.37}$$

Since $\prod_{p=1}^{k-1} |\hat{h}(2^{-p}\omega)|^2\, \mathrm{e}^{in\omega}$ is $2^k\pi$ periodic we obtain $I_k[n] = I_{k-1}[n]$, and by induction $I_k[n] = I_1[n]$. Writing (7.37) for $k = 1$ gives

$$I_1[n] = \int_{0}^{2\pi} \mathrm{e}^{in\omega}\, d\omega = 2\pi\, \delta[n],$$

which verifies that $I_k[n] = 2\pi\delta[n]$, for all $k \geqslant 1$.

We shall now prove that $\hat{\phi} \in \mathbf{L^2}(\mathbb{R})$. For all $\omega \in \mathbb{R}$

$$\lim_{k\to\infty} |\hat{\phi}_k(\omega)|^2 = \prod_{p=1}^{\infty} \frac{|\hat{h}(2^{-p}\omega)|^2}{2} = |\hat{\phi}(\omega)|^2.$$

The Fatou Lemma A.1 on positive functions proves that

$$\int_{-\infty}^{+\infty} |\hat{\phi}(\omega)|^2 \, d\omega \leqslant \lim_{k \to \infty} \int_{-\infty}^{+\infty} |\hat{\phi}_k(\omega)|^2 \, d\omega = 2\pi, \tag{7.38}$$

because $I_k[0] = 2\pi$ for all $k \geqslant 1$. Since

$$|\hat{\phi}(\omega)|^2 \, \mathrm{e}^{in\omega} = \lim_{k \to \infty} |\hat{\phi}_k(\omega)|^2 \, \mathrm{e}^{in\omega} \ ,$$

we finally verify that

$$\int_{-\infty}^{+\infty} |\hat{\phi}(\omega)|^2 \, \mathrm{e}^{in\omega} \, d\omega = \lim_{k \to \infty} \int_{-\infty}^{+\infty} |\hat{\phi}_k(\omega)|^2 \, \mathrm{e}^{in\omega} \, d\omega = 2\pi \, \delta[n] \tag{7.39}$$

by applying the dominated convergence Theorem A.1. This requires verifying the upper-bound condition (A.1). This is done in our case by proving the existence of a constant C such that

$$\left| |\hat{\phi}_k(\omega)|^2 \, \mathrm{e}^{in\omega} \right| = |\hat{\phi}_k(\omega)|^2 \leqslant C \, |\hat{\phi}(\omega)|^2. \tag{7.40}$$

Indeed, we showed in (7.38) that $|\hat{\phi}(\omega)|^2$ is an integrable function.

The existence of $C > 0$ satisfying (7.40) is trivial for $|\omega| > 2^k\pi$ since $\hat{\phi}_k(\omega) = 0$. For $|\omega| \leqslant 2^k\pi$ since $\hat{\phi}(\omega) = 2^{-1/2} \, \hat{h}(\omega/2) \, \hat{\phi}(\omega/2)$, it follows that

$$|\hat{\phi}(\omega)|^2 = |\hat{\phi}_k(\omega)|^2 \, |\hat{\phi}(2^{-k}\omega)|^2.$$

To prove (7.40) for $|\omega| \leqslant 2^k\pi$, it is therefore sufficient to show that $|\hat{\phi}(\omega)|^2 \geqslant 1/C$ for $\omega \in [-\pi, \pi]$.

Let us first study the neighborhood of $\omega = 0$. Since $\hat{h}(\omega)$ is continuously differentiable in this neighborhood and since $|\hat{h}(\omega)|^2 \leqslant 2 = |\hat{h}(0)|^2$, the functions $|\hat{h}(\omega)|^2$ and $\log_{\mathrm{e}} |\hat{h}(\omega)|^2$ have derivatives that vanish at $\omega = 0$. It follows that there exists $\varepsilon > 0$ such that

$$\forall |\omega| \leqslant \varepsilon \ \ , \ \ 0 \geqslant \log_{\mathrm{e}} \left(\frac{|\hat{h}(\omega)|^2}{2} \right) \geqslant -|\omega|.$$

Hence, for $|\omega| \leqslant \varepsilon$

$$|\hat{\phi}(\omega)|^2 = \exp \left[\sum_{p=1}^{+\infty} \log_{\mathrm{e}} \left(\frac{|\hat{h}(2^{-p}\omega)|^2}{2} \right) \right] \geqslant \mathrm{e}^{-|\omega|} \geqslant \mathrm{e}^{-\varepsilon}. \tag{7.41}$$

Now let us analyze the domain $|\omega| > \varepsilon$. To do this we take an integer l such that $2^{-l}\pi < \varepsilon$. Condition (7.31) proves that $K = \inf_{\omega \in [-\pi/2, \pi/2]} |\hat{h}(\omega)| > 0$ so if $|\omega| \leqslant \pi$

$$|\hat{\phi}(\omega)|^2 = \prod_{p=1}^{l} \frac{|\hat{h}(2^{-p}\omega)|^2}{2} \left| \hat{\phi}\left(2^{-l}\omega\right) \right|^2 \geqslant \frac{K^{2l}}{2^l} \, \mathrm{e}^{-\varepsilon} = \frac{1}{C}.$$

This last result finishes the proof of inequality (7.40). Applying the dominated convergence Theorem A.1 proves (7.39) and hence that $\{\phi(t-n)\}_{n \in \mathbb{Z}}$ is orthonormal. A simple change of variable shows that $\{\phi_{j,n}\}_{j \in \mathbb{Z}}$ is orthonormal for all $j \in \mathbb{Z}$.

• *Proof that* $\{\mathbf{V}_j\}_{j \in \mathbb{Z}}$ *is a multiresolution.* To verify that ϕ is a scaling function, we must show that the spaces $\mathbf{V}_j$ generated by $\{\phi_{j,n}\}_{j \in \mathbb{Z}}$ define a multiresolution approximation. The multiresolution properties (7.1) and (7.3) are clearly true. The causality $\mathbf{V}_{j+1} \subset \mathbf{V}_j$ is verified by showing that for any $p \in \mathbb{Z}$,

$$\phi_{j+1,p} = \sum_{n=-\infty}^{+\infty} h[n - 2p] \, \phi_{j,n}.$$

This equality is proved later in (7.107). Since all vectors of a basis of $\mathbf{V}_{j+1}$ can decomposed in a basis of $\mathbf{V}_j$ it follows that $\mathbf{V}_{j+1} \subset \mathbf{V}_j$.

To prove the multiresolution property (7.4) we must show that any $f \in \mathbf{L^2}(\mathbb{R})$ satisfies

$$\lim_{j \to +\infty} \| P_{\mathbf{V}_j} f \| = 0. \tag{7.42}$$

Since $\{\phi_{j,n}\}_{n \in \mathbb{Z}}$ is an orthonormal basis of $\mathbf{V}_j$

$$\| P_{\mathbf{V}_j} f \|^2 = \sum_{n=-\infty}^{+\infty} |\langle f, \phi_{j,n} \rangle|^2.$$

Suppose first that f is bounded by A and has a compact support included in $[2^J, 2^J]$. The constants A and J may be arbitrarily large. It follows that

$$\begin{aligned}\sum_{n=-\infty}^{+\infty} |\langle f, \phi_{j,n}\rangle|^2 &\leqslant 2^{-j}\left[\sum_{n=-\infty}^{+\infty}\int_{-2^J}^{2^J} |f(t)|\,|\phi(2^{-j}t-n)|\,dt\right]^2\\ &\leqslant 2^{-j}A^2\left[\sum_{n=-\infty}^{+\infty}\int_{-2^J}^{2^J} |\phi(2^{-j}t-n)|\,dt\right]^2\end{aligned}$$

Applying the Cauchy-Schwarz inequality to $1\times|\phi(2^{-j}t-n)|$ yields

$$\begin{aligned}\sum_{n=-\infty}^{+\infty} |\langle f, \phi_{j,n}\rangle|^2 &\leqslant A^2\,2^{J+1}\sum_{n=-\infty}^{+\infty}\int_{-2^J}^{2^J} |\phi(2^{-j}t-n)|^2\,2^{-j}\,dt\\ &\leqslant A^2 2^{J+1}\int_{S_j}|\phi(t)|^2\,dt = A^2\,2^{J+1}\int_{-\infty}^{+\infty}|\phi(t)|^2\,\mathbf{1}_{S_j}(t)\,dt,\end{aligned}$$

with $S_j = \cup_{n\in\mathbb{Z}}[n-2^{J-j}, n+2^{J-j}]$ for $j>J$. For $t\notin\mathbb{Z}$ we obviously have $\mathbf{1}_{S_j}(t)\to 0$ for $j\to+\infty$. The dominated convergence Theorem A.1 applied to $|\phi(t)|^2\,\mathbf{1}_{S_j}(t)$ proves that the integral converges to 0 and hence

$$\lim_{j\to+\infty}\sum_{n=-\infty}^{+\infty}|\langle f,\phi_{j,n}\rangle|^2 = 0.$$

Property (7.42) is extended to any $f\in\mathbf{L^2}(\mathbb{R})$ by using the density in $\mathbf{L^2}(\mathbb{R})$ of bounded function with a compact support, and Theorem A.5.

To prove the last multiresolution property (7.5) we must show that for any $f\in\mathbf{L^2}(\mathbb{R})$,

$$\lim_{j\to-\infty}\|f-P_{\mathbf{V}_j}f\|^2 = \lim_{j\to-\infty}\left(\|f\|^2-\|P_{\mathbf{V}_j}f\|^2\right)=0. \tag{7.43}$$

We consider functions f whose Fourier transform $\hat f$ has a compact support included in $[-2^J\pi, 2^J\pi]$ for J large enough. We proved in (7.36) that the Fourier transform of $P_{\mathbf{V}_j}f$ is

$$\widehat{P_{\mathbf{V}_j}f}(\omega) = \hat\phi(2^j\omega)\sum_{k=-\infty}^{+\infty}\hat f\left(\omega-2^{-j}2k\pi\right)\,\hat\phi^*\left(2^j\left[\omega-2^{-j}2k\pi\right]\right).$$

If $j<-J$, then the supports of $\hat f(\omega-2^{-j}2k\pi)$ are disjoint for different k so

$$\begin{aligned}\|P_{\mathbf{V}_j}f\|^2 &= \frac{1}{2\pi}\int_{-\infty}^{+\infty}|\hat f(\omega)|^2\,|\hat\phi(2^j\omega)|^4\,d\omega \\ &\quad+\frac{1}{2\pi}\int_{-\infty}^{+\infty}\sum_{\substack{k=-\infty\\k\neq0}}^{+\infty}|\hat f\left(\omega-2^{-j}2k\pi\right)|^2\,|\hat\phi(2^j\omega)|^2\,|\hat\phi\left(2^j\left[\omega-2^{-j}2k\pi\right]\right)|^2\,d\omega.\end{aligned} \tag{7.44}$$

We have already observed that $|\phi(\omega)|\leqslant 1$ and (7.41) proves that for ω sufficiently small $|\phi(\omega)|\geqslant \mathrm{e}^{-|\omega|}$ so

$$\lim_{\omega\to0}|\hat\phi(\omega)| = 1.$$

Since $|\hat f(\omega)|^2|\hat\phi(2^j\omega)|^4\leqslant|\hat f(\omega)|^2$ and $\lim_{j\to-\infty}|\hat\phi(2^j\omega)|^4|\hat f(\omega)|^2=|\hat f(\omega)|^2$ one can apply the dominated convergence Theorem A.1, to prove that

$$\lim_{j\to-\infty}\int_{-\infty}^{+\infty}|\hat f(\omega)|^2\,|\hat\phi(2^j\omega)|^4\,d\omega = \int_{-\infty}^{+\infty}|\hat f(\omega)|^2\,d\omega = \|f\|^2. \tag{7.45}$$

The operator $P_{\mathbf{V}_j}$ is an orthogonal projector, so $\|P_{\mathbf{V}_j}f\|\leqslant\|f\|$. With (7.44) and (7.45), this implies that $\lim_{j\to-\infty}(\|f\|^2-\|P_{\mathbf{V}_j}f\|^2)=0$, and hence verifies (7.43). This property is extended to any $f\in\mathbf{L^2}(\mathbb{R})$ by using the density in $\mathbf{L^2}(\mathbb{R})$ of functions whose Fourier transforms have a compact support and the result of Theorem A.5. ■

Discrete filters whose transfer functions satisfy (7.29) are called *conjugate mirror filters*. As we shall see in Section 7.3, they play an important role in discrete signal processing; they make it possible to decompose discrete signals in separate frequency bands with filter banks. One difficulty

of the proof is showing that the infinite cascade of convolutions that is represented in the Fourier domain by the product (7.32) does converge to a decent function in $\mathbf{L^2}(\mathbb{R})$. The sufficient condition (7.31) is not necessary to construct a scaling function, but it is always satisfied in practical designs of conjugate mirror filters. It cannot just be removed as shown by the example $\hat{h}(\omega) = \cos(3\omega/2)$, which satisfies all other conditions. In this case, a simple calculation shows that $\phi = 1/3\,\mathbf{1}_{[-3/2,3/2]}$. Clearly $\{\phi(t-n)\}_{n\in\mathbb{Z}}$ is not orthogonal so ϕ is not a scaling function. The condition (7.31) may however be replaced by a weaker but more technical necessary and sufficient condition proved by Cohen [15, 166].

Example 7.6. *For a Shannon multiresolution approximation, $\hat{\phi} = \mathbf{1}_{[-\pi,\pi]}$. We thus derive from (7.32) that*

$$\forall \omega \in [-\pi,\pi] \quad , \quad \hat{h}(\omega) = \sqrt{2}\,\mathbf{1}_{[-\pi/2,\pi/2]}(\omega).$$

Example 7.7. *For piecewise constant approximations, $\phi = \mathbf{1}_{[0,1]}$. Since $h[n] = \langle 2^{-1/2}\phi(t/2), \phi(t-n)\rangle$ it follows that*

$$h[n] = \begin{cases} 2^{-1/2} & \text{if } n = 0, 1 \\ 0 & \text{otherwise} \end{cases} \tag{7.46}$$

Example 7.8. *Polynomial splines of degree m correspond to a conjugate mirror filter $\hat{h}(\omega)$ that is calculated from $\hat{\phi}(\omega)$ with (7.25):*

$$\hat{h}(\omega) = \sqrt{2}\,\frac{\hat{\phi}(2\omega)}{\hat{\phi}(\omega)}. \tag{7.47}$$

Inserting (7.18) yields

$$\hat{h}(\omega) = \exp\left(\frac{-i\varepsilon\omega}{2}\right)\sqrt{\frac{S_{2m+2}(\omega)}{2^{2m+1}\,S_{2m+2}(2\omega)}}, \tag{7.48}$$

where $\varepsilon = 0$ if m is odd and $\varepsilon = 1$ if m is even. For linear splines $m = 1$ so (7.20) implies that

$$\hat{h}(\omega) = \sqrt{2}\,\left[\frac{1+2\cos^2(\omega/2)}{1+2\cos^2\omega}\right]^{1/2}\cos^2\left(\frac{\omega}{2}\right). \tag{7.49}$$

For cubic splines, the conjugate mirror filter is calculated by inserting (7.22) in (7.48). Figure 7.4 gives the graph of $|\hat{h}(\omega)|^2$. The impulse responses $h[n]$ of these filters have an infinite support but an exponential decay. For m odd, $h[n]$ is symmetric about $n = 0$. Table 7.1 gives the coefficients $h[n]$ above 10^{-4} for $m = 1, 3$.

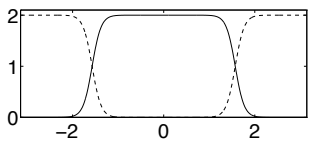

Figure 7.4: The solid line gives $|\hat{h}(\omega)|^2$ on $[-\pi,\pi]$, for a cubic spline multiresolution. The dotted line corresponds to $|\hat{g}(\omega)|^2$.

7.1.4 In Which Orthogonal Wavelets Finally Arrive

Orthonormal wavelets carry the details necessary to increase the resolution of a signal approximation. The approximations of f at the scales 2^j and 2^{j-1} are respectively equal to their orthogonal projections on $\mathbf{V}_j$ and $\mathbf{V}_{j-1}$. We know that $\mathbf{V}_j$ is included in $\mathbf{V}_{j-1}$. Let $\mathbf{W}_j$ be the orthogonal complement of $\mathbf{V}_j$ in $\mathbf{V}_{j-1}$:

$$\mathbf{V}_{j-1} = \mathbf{V}_j \oplus \mathbf{W}_j. \tag{7.50}$$

	n	$h[n]$		n	$h[n]$
$m=1$	0	0.817645956	$m=3$	$5,-5$	0.042068328
	$1,-1$	0.397296430		$6,-6$	−0.017176331
	$2,-2$	−0.069101020		$7,-7$	−0.017982291
	$3,-3$	−0.051945337		$8,-8$	0.008685294
	$4,-4$	0.016974805		$9,-9$	0.008201477
	$5,-5$	0.009990599		$10,-10$	−0.004353840
	$6,-6$	−0.003883261		$11,-11$	−0.003882426
	$7,-7$	−0.002201945		$12,-12$	0.002186714
	$8,-8$	0.000923371		$13,-13$	0.001882120
	$9,-9$	0.000511636		$14,-14$	−0.001103748
	$10,-10$	−0.000224296		$15,-15$	−0.000927187
	$11,-11$	−0.000122686		$16,-16$	0.000559952
$m=3$	0	0.766130398		$17,-17$	0.000462093
	$1,-1$	0.433923147		$18,-18$	−0.000285414
	$2,-2$	−0.050201753		$19,-19$	−0.000232304
	$3,-3$	−0.110036987		$20,-20$	0.000146098
	$4,-4$	0.032080869			

Table 7.1: Conjugate mirror filters $h[n]$ corresponding to linear splines $m=1$ and cubic splines $m=3$. The coefficients below 10^{-4} are not given.

The orthogonal projection of f on $\mathbf{V}_{j-1}$ can be decomposed as the sum of orthogonal projections on $\mathbf{V}_j$ and $\mathbf{W}_j$:

$$P_{\mathbf{V}_{j-1}} f = P_{\mathbf{V}_j} f + P_{\mathbf{W}_j} f. \tag{7.51}$$

The complement $P_{\mathbf{W}_j} f$ provides the "details" of f that appear at the scale 2^{j-1} but which disappear at the coarser scale 2^j. The following theorem [43, 361] proves that one can construct an orthonormal basis of $\mathbf{W}_j$ by scaling and translating a wavelet ψ.

Theorem 7.3 (Mallat, Meyer)**.** *Let ϕ be a scaling function and h the corresponding conjugate mirror filter. Let ψ be the function whose Fourier transform is*

$$\hat{\psi}(\omega) = \frac{1}{\sqrt{2}}\, \hat{g}\left(\frac{\omega}{2}\right) \hat{\phi}\left(\frac{\omega}{2}\right), \tag{7.52}$$

with

$$\hat{g}(\omega) = \mathrm{e}^{-i\omega}\, \hat{h}^*(\omega + \pi). \tag{7.53}$$

Let us denote

$$\psi_{j,n}(t) = \frac{1}{\sqrt{2^j}}\, \psi\left(\frac{t - 2^j n}{2^j}\right).$$

For any scale 2^j, $\{\psi_{j,n}\}_{n\in\mathbb{Z}}$ is an orthonormal basis of $\mathbf{W}_j$. For all scales, $\{\psi_{j,n}\}_{(j,n)\in\mathbb{Z}^2}$ is an orthonormal basis of $\mathbf{L^2}(\mathbb{R})$.

Proof. Let us prove first that $\hat{\psi}$ can be written as the product (7.52). Necessarily $\psi(t/2) \in \mathbf{W}_1 \subset \mathbf{V}_0$. It can thus be decomposed in $\{\phi(t-n)\}_{n\in\mathbb{Z}}$ which is an orthogonal basis of $\mathbf{V}_0$:

$$\frac{1}{\sqrt{2}}\, \psi\left(\frac{t}{2}\right) = \sum_{n=-\infty}^{+\infty} g[n]\, \phi(t-n), \tag{7.54}$$

with

$$g[n] = \frac{1}{\sqrt{2}} \left\langle \psi\left(\frac{t}{2}\right), \phi(t-n) \right\rangle. \tag{7.55}$$

The Fourier transform of (7.54) yields

$$\hat{\psi}(2\omega) = \frac{1}{\sqrt{2}}\, \hat{g}(\omega)\, \hat{\phi}(\omega). \tag{7.56}$$

The following lemma gives necessary and sufficient conditions on $\hat{g}$ for designing an orthogonal wavelet.

Lemma 7.1. *The family $\{\psi_{j,n}\}_{n\in\mathbb{Z}}$ is an orthonormal basis of $\mathbf{W}_j$ if and only if*

$$|\hat{g}(\omega)|^2 + |\hat{g}(\omega+\pi)|^2 = 2 \tag{7.57}$$

and

$$\hat{g}(\omega)\,\hat{h}^*(\omega) + \hat{g}(\omega+\pi)\,\hat{h}^*(\omega+\pi) = 0. \tag{7.58}$$

The lemma is proved for $j = 0$ from which it is easily extended to $j \neq 0$ with an appropriate scaling. As in (7.14) one can verify that $\{\psi(t-n)\}_{n\in\mathbb{Z}}$ is orthonormal if and only if

$$\forall \omega \in \mathbb{R} \;\;,\;\; I(\omega) = \sum_{k=-\infty}^{+\infty} |\hat{\psi}(\omega+2k\pi)|^2 = 1. \tag{7.59}$$

Since $\hat{\psi}(\omega) = 2^{-1/2}\,\hat{g}(\omega/2)\,\hat{\phi}(\omega/2)$ and $\hat{g}(\omega)$ is 2π periodic,

$$\begin{aligned} I(\omega) &= \sum_{k=-\infty}^{+\infty} |\hat{g}\left(\frac{\omega}{2}+k\pi\right)|^2\,|\hat{\phi}\left(\frac{\omega}{2}+k\pi\right)|^2 \\ &= |\hat{g}\Big(\frac{\omega}{2}\Big)|^2 \sum_{p=-\infty}^{+\infty} |\hat{\phi}\Big(\frac{\omega}{2}+2p\pi\Big)|^2 + |\hat{g}\Big(\frac{\omega}{2}+\pi\Big)|^2 \sum_{p=-\infty}^{+\infty} |\hat{\phi}\Big(\frac{\omega}{2}+\pi+2p\pi\Big)|^2. \end{aligned}$$

We know that $\sum_{p=-\infty}^{+\infty} |\hat{\phi}(\omega+2p\pi)|^2 = 1$ so (7.59) is equivalent to (7.57).

The space $\mathbf{W}_0$ is orthogonal to $\mathbf{V}_0$ if and only if $\{\phi(t-n)\}_{n\in\mathbb{Z}}$ and $\{\psi(t-n)\}_{n\in\mathbb{Z}}$ are orthogonal families of vectors. This means that for any $n \in \mathbb{Z}$

$$\langle \psi(t), \phi(t-n)\rangle = \psi \star \bar{\phi}(n) = 0.$$

The Fourier transform of $\psi \star \bar{\phi}(t)$ is $\hat{\psi}(\omega)\hat{\phi}^*(\omega)$. The sampled sequence $\psi \star \bar{\phi}(n)$ is zero if its Fourier series computed with (3.3) satisfies

$$\forall \omega \in \mathbb{R} \;\;,\;\; \sum_{k=-\infty}^{+\infty} \hat{\psi}(\omega+2k\pi)\,\hat{\phi}^*(\omega+2k\pi) = 0. \tag{7.60}$$

By inserting $\hat{\psi}(\omega) = 2^{-1/2}\,\hat{g}(\omega/2)\,\hat{\phi}(\omega/2)$ and $\hat{\phi}(\omega) = 2^{-1/2}\,\hat{h}(\omega/2)\,\hat{\phi}(\omega/2)$ in this equation, since $\sum_{k=-\infty}^{+\infty} |\hat{\phi}(\omega+2k\pi)|^2 = 1$ we prove as before that (7.60) is equivalent to (7.58).

We must finally verify that $\mathbf{V}_{-1} = \mathbf{V}_0 \oplus \mathbf{W}_0$. Knowing that $\{\sqrt{2}\phi(2t-n)\}_{n\in\mathbb{Z}}$ is an orthogonal basis of $\mathbf{V}_{-1}$, it is equivalent to show that for any $a[n] \in \ell^2(\mathbb{Z})$ there exist $b[n] \in \ell^2(\mathbb{Z})$ and $c[n] \in \ell^2(\mathbb{Z})$ such that

$$\sum_{n=-\infty}^{+\infty} a[n]\,\sqrt{2}\,\phi(2[t-2^{-1}n]) = \sum_{n=-\infty}^{+\infty} b[n]\,\phi(t-n) + \sum_{n=-\infty}^{+\infty} c[n]\,\psi(t-n). \tag{7.61}$$

This is done by relating $\hat{b}(\omega)$ and $\hat{c}(\omega)$ to $\hat{a}(\omega)$. The Fourier transform of (7.61) yields

$$\frac{1}{\sqrt{2}}\,\hat{a}\left(\frac{\omega}{2}\right)\hat{\phi}\left(\frac{\omega}{2}\right) = \hat{b}(\omega)\,\hat{\phi}(\omega) + \hat{c}(\omega)\,\hat{\psi}(\omega).$$

Inserting $\hat{\psi}(\omega) = 2^{-1/2}\,\hat{g}(\omega/2)\,\hat{\phi}(\omega/2)$ and $\hat{\phi}(\omega) = 2^{-1/2}\,\hat{h}(\omega/2)\,\hat{\phi}(\omega/2)$ in this equation shows that it is necessarily satisfied if

$$\hat{a}\left(\frac{\omega}{2}\right) = \hat{b}(\omega)\,\hat{h}\left(\frac{\omega}{2}\right) + \hat{c}(\omega)\,\hat{g}\left(\frac{\omega}{2}\right). \tag{7.62}$$

Let us define

$$\hat{b}(2\omega) = \frac{1}{2}\,[\hat{a}(\omega)\,\hat{h}^*(\omega) + \hat{a}(\omega+\pi)\,\hat{h}^*(\omega+\pi)]$$

and

$$\hat{c}(2\omega) = \frac{1}{2}\,[\hat{a}(\omega)\,\hat{g}^*(\omega) + \hat{a}(\omega+\pi)\,\hat{g}^*(\omega+\pi)].$$

When calculating the right-hand side of (7.62) we verify that it is equal to the left-hand side by inserting (7.57), (7.58) and using

$$|\hat{h}(\omega)|^2 + |\hat{h}(\omega+\pi)|^2 = 2. \tag{7.63}$$

Since $\hat{b}(\omega)$ and $\hat{c}(\omega)$ are 2π periodic they are the Fourier series of two sequences $b[n]$ and $c[n]$ that satisfy (7.61). This finishes the proof of the lemma.

The formula (7.53)

$$\hat{g}(\omega) = \mathrm{e}^{-i\omega}\, \hat{h}^*(\omega + \pi)$$

satisfies (7.57) and (7.58) because of (7.63). We thus derive from Lemma 7.1 that $\{\psi_{j,n}\}_{(j,n)\in\mathbb{Z}^2}$ is an orthogonal basis of $\mathbf{W}_j$.

We complete the proof of the theorem by verifying that $\{\psi_{j,n}\}_{(j,n)\in\mathbb{Z}^2}$ is an orthogonal basis of $\mathbf{L^2}(\mathbb{R})$. Observe first that the detail spaces $\{\mathbf{W}_j\}_{j\in\mathbb{Z}}$ are orthogonal. Indeed $\mathbf{W}_j$ is orthogonal to $\mathbf{V}_j$ and $\mathbf{W}_l \subset \mathbf{V}_{l-1} \subset \mathbf{V}_j$ for $j < l$. Hence $\mathbf{W}_j$ and $\mathbf{W}_l$ are orthogonal. We can also decompose

$$\mathbf{L^2}(\mathbb{R}) = \oplus_{j=-\infty}^{+\infty} \mathbf{W}_j. \tag{7.64}$$

Indeed $\mathbf{V}_{j-1} = \mathbf{W}_j \oplus \mathbf{V}_j$ and we verify by substitution that for any $L > J$

$$\mathbf{V}_L = \oplus_{j=L-1}^{J} \mathbf{W}_j \,\oplus\, \mathbf{V}_J. \tag{7.65}$$

Since $\{\mathbf{V}_j\}_{j\in\mathbb{Z}}$ is a multiresolution approximation, $\mathbf{V}_L$ and $\mathbf{V}_J$ tend respectively to $\mathbf{L^2}(\mathbb{R})$ and $\{0\}$ when L and J go respectively to $-\infty$ and $+\infty$, which implies (7.64). A union of orthonormal bases of all $\mathbf{W}_j$ is therefore an orthonormal basis of $\mathbf{L^2}(\mathbb{R})$. ■ ■

The proof of the theorem shows that $\hat{g}$ is the Fourier series of

$$g[n] = \left\langle \frac{1}{\sqrt{2}} \psi\left(\frac{t}{2}\right), \phi(t-n) \right\rangle, \tag{7.66}$$

which are the decomposition coefficients of

$$\frac{1}{\sqrt{2}}\, \psi\left(\frac{t}{2}\right) = \sum_{n=-\infty}^{+\infty} g[n]\, \phi(t-n). \tag{7.67}$$

Calculating the inverse Fourier transform of (7.53) yields

$$g[n] = (-1)^{1-n}\, h[1-n]. \tag{7.68}$$

This mirror filter plays an important role in the fast wavelet transform algorithm.

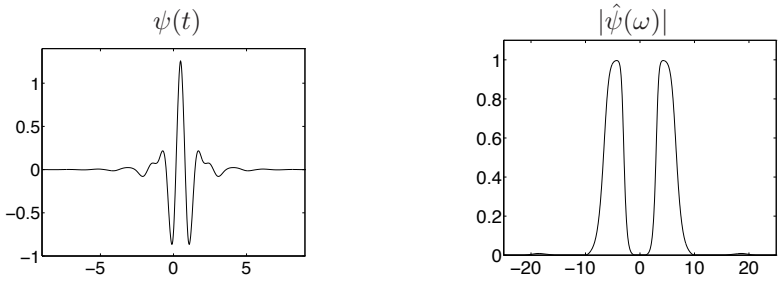

Figure 7.5: Battle-Lemarié cubic spline wavelet ψ and its Fourier transform modulus.

Example 7.9. *Figure 7.5 displays the cubic spline wavelet ψ and its Fourier transform $\hat{\psi}$ calculated by inserting in (7.52) the expressions (7.18) and (7.48) of $\hat{\phi}(\omega)$ and $\hat{h}(\omega)$. The properties of this Battle-Lemarié spline wavelet are further studied in Section 7.2.2. Like most orthogonal wavelets, the energy of $\hat{\psi}$ is essentially concentrated in $[-2\pi, -\pi] \cup [\pi, 2\pi]$. For any ψ that generates an orthogonal basis of $\mathbf{L^2}(\mathbb{R})$, one can verify that*

$$\forall \omega \in \mathbb{R} - \{0\} \quad , \quad \sum_{j=-\infty}^{+\infty} |\hat{\psi}(2^j\omega)|^2 = 1.$$

This is illustrated in Figure 7.6.

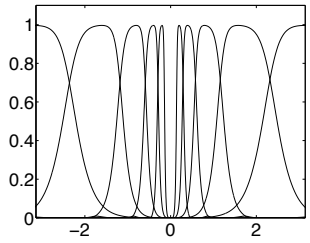

Figure 7.6: Graphs of $|\hat{\psi}(2^j\omega)|^2$ for the cubic spline Battle-Lemarié wavelet, with $1 \leqslant j \leqslant 5$ and $\omega \in [-\pi, \pi]$.

The orthogonal projection of a signal f in a "detail" space $\mathbf{W}_j$ is obtained with a partial expansion in its wavelet basis

$$P_{\mathbf{W}_j} f = \sum_{n=-\infty}^{+\infty} \langle f, \psi_{j,n} \rangle \, \psi_{j,n}.$$

A signal expansion in a wavelet orthogonal basis can thus be viewed as an aggregation of details at all scales 2^j that go from 0 to $+\infty$

$$f = \sum_{j=-\infty}^{+\infty} P_{\mathbf{W}_j} f = \sum_{j=-\infty}^{+\infty} \sum_{n=-\infty}^{+\infty} \langle f, \psi_{j,n} \rangle \, \psi_{j,n}.$$

Figure 7.7 gives the coefficients of a signal decomposed in the cubic spline wavelet orthogonal basis. The calculations are performed with the fast wavelet transform algorithm of Section 7.3. The up or down Diracs give the amplitudes of positive or negative wavelet coefficients, at a distance $2^j n$ at each scale 2^j. Coefficients are nearly zero at fine scales where the signal is locally regular.

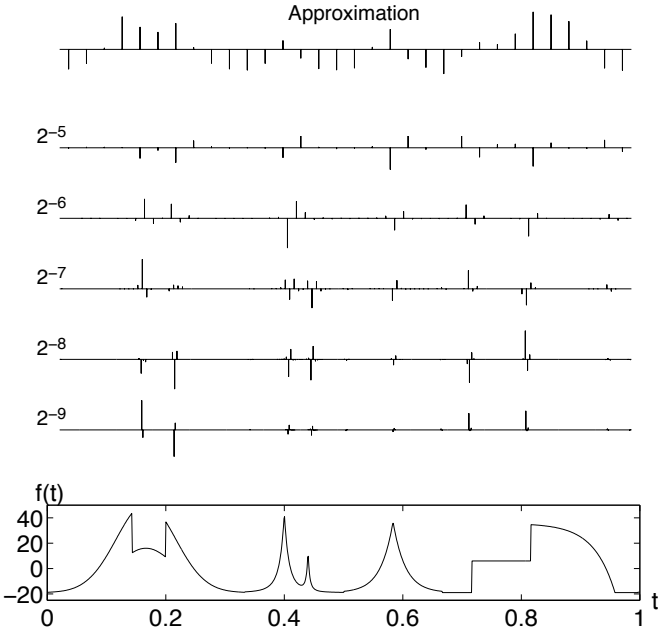

Figure 7.7: Wavelet coefficients $d_j[n] = \langle f, \psi_{j,n} \rangle$ calculated at scales 2^j with the cubic spline wavelet. Each up or down Dirac gives the amplitude of a positive or negative wavelet coefficient. At the top is the remaining coarse signal approximation $a_J[n] = \langle f, \phi_{J,n} \rangle$ for $J = -5$.

Wavelet Design Theorem 7.3 constructs a wavelet orthonormal basis from any conjugate mirror filter $\hat{h}(\omega)$. This gives a simple procedure for designing and building wavelet orthogonal bases.

Conversely, we may wonder whether all wavelet orthonormal bases are associated to a multiresolution approximation and a conjugate mirror filter. If we impose that ψ has a compact support then Lemarié [51] proved that ψ necessarily corresponds to a multiresolution approximation. It is however possible to construct pathological wavelets that decay like $|t|^{-1}$ at infinity, and which cannot be derived from any multiresolution approximation. Section 7.2 describes important classes of wavelet bases and explains how to design $\hat{h}$ to specify the support, the number of vanishing moments and the regularity of ψ.

7.2 Classes of Wavelet Bases

7.2.1 Choosing a Wavelet

Most applications of wavelet bases exploit their ability to efficiently approximate particular classes of functions with few non-zero wavelet coefficients. This is true not only for data compression but also for noise removal and fast calculations. The design of ψ must therefore be optimized to produce a maximum number of wavelet coefficients $\langle f, \psi_{j,n}\rangle$ that are close to zero. A function f has few non-negligible wavelet coefficients if most of the fine-scale (high-resolution) wavelet coefficients are small. This depends mostly on the regularity of f, the number of vanishing moments of ψ and the size of its support. To construct an appropriate wavelet from a conjugate mirror filter $h[n]$, we relate these properties to conditions on $\hat{h}(\omega)$.

Vanishing Moments Let us recall that ψ has p vanishing moments if

$$\int_{-\infty}^{+\infty} t^k\, \psi(t)\, dt = 0 \quad \text{for } 0 \leqslant k < p. \tag{7.69}$$

This means that ψ is orthogonal to any polynomial of degree $p-1$. Section 6.1.3 proves that if f is regular and ψ has enough vanishing moments then the wavelet coefficients $|\langle f, \psi_{j,n}\rangle|$ are small at fine scales 2^j. Indeed, if f is locally $\mathbf{C}^k$, then over a small interval it is well approximated by a Taylor polynomial of degree k. If $k < p$, then wavelets are orthogonal to this Taylor polynomial and thus produce small amplitude coefficients at fine scales. The following theorem relates the number of vanishing moments of ψ to the vanishing derivatives of $\hat{\psi}(\omega)$ at $\omega = 0$ and to the number of zeroes of $\hat{h}(\omega)$ at $\omega = \pi$. It also proves that polynomials of degree $p-1$ are then reproduced by the scaling functions.

Theorem 7.4 (Vanishing moments). *Let ψ and ϕ be a wavelet and a scaling function that generate an orthogonal basis. Suppose that $|\psi(t)| = O((1+t^2)^{-p/2-1})$ and $|\phi(t)| = O((1+t^2)^{-p/2-1})$. The four following statements are equivalent:*

(i) The wavelet ψ has p vanishing moments.
(ii) $\hat{\psi}(\omega)$ and its first $p-1$ derivatives are zero at $\omega = 0$.
(iii) $\hat{h}(\omega)$ and its first $p-1$ derivatives are zero at $\omega = \pi$.
(iv) For any $0 \leqslant k < p$,

$$q_k(t) = \sum_{n=-\infty}^{+\infty} n^k\, \phi(t-n) \quad \textit{is a polynomial of degree } k. \tag{7.70}$$

Proof. The decay of $|\phi(t)|$ and $|\psi(t)|$ implies that $\hat{\psi}(\omega)$ and $\hat{\phi}(\omega)$ are p times continuously differentiable. The k^{th} order derivative $\hat{\psi}^{(k)}(\omega)$ is the Fourier transform of $(-it)^k \psi(t)$. Hence

$$\hat{\psi}^{(k)}(0) = \int_{-\infty}^{+\infty} (-it)^k\, \psi(t)\, dt.$$

We derive that (i) is equivalent to (ii).

Theorem 7.3 proves that

$$\sqrt{2}\, \hat{\psi}(2\omega) = \mathrm{e}^{-i\omega}\, \hat{h}^*(\omega+\pi)\, \hat{\phi}(\omega).$$

Since $\hat{\phi}(0) \neq 0$, by differentiating this expression we prove that (ii) is equivalent to (iii).

Let us now prove that (iv) implies (i). Since ψ is orthogonal to $\{\phi(t-n)\}_{n\in\mathbb{Z}}$, it is thus also orthogonal to the polynomials q_k for $0 \leqslant k < p$. This family of polynomials is a basis of the space of polynomials of degree at most $p-1$. Hence ψ is orthogonal to any polynomial of degree $p-1$ and in particular to t^k for $0 \leqslant k < p$. This means that ψ has p vanishing moments.

To verify that (i) implies (iv) we suppose that ψ has p vanishing moments, and for $k < p$ we evaluate $q_k(t)$ defined in (7.70). This is done by computing its Fourier transform:

$$\hat{q}_k(\omega) = \hat{\phi}(\omega) \sum_{n=-\infty}^{+\infty} n^k \exp(-in\omega) = (i)^k \hat{\phi}(\omega) \frac{d^k}{d\omega^k} \sum_{n=-\infty}^{+\infty} \exp(-in\omega) \ .$$

Let $\delta^{(k)}$ be the distribution that is the k^{th} order derivative of a Dirac, defined in Appendix A.7. The Poisson formula (2.4) proves that

$$\hat{q}_k(\omega) = (i)^k \frac{1}{2\pi} \hat{\phi}(\omega) \sum_{l=-\infty}^{+\infty} \delta^{(k)}(\omega - 2l\pi). \tag{7.71}$$

With several integrations by parts, we verify the distribution equality

$$\hat{\phi}(\omega)\, \delta^{(k)}(\omega - 2l\pi) = \hat{\phi}(2l\pi)\, \delta^{(k)}(\omega - 2l\pi) + \sum_{m=0}^{k-1} a_{m,l}^k\, \delta^{(m)}(\omega - 2l\pi), \tag{7.72}$$

where $a_{m,l}^k$ is a linear combination of the derivatives $\{\hat{\phi}^{(m)}(2l\pi)\}_{0\leqslant m\leqslant k}$.

For $l \neq 0$, let us prove that $a_{m,l}^k = 0$ by showing that $\hat{\phi}^{(m)}(2l\pi) = 0$ if $0 \leqslant m < p$. For any $P > 0$, (7.27) implies

$$\hat{\phi}(\omega) = \hat{\phi}(2^{-P}\omega) \prod_{p=1}^{P} \frac{\hat{h}(2^{-p}\omega)}{\sqrt{2}}. \tag{7.73}$$

Since ψ has p vanishing moments, we showed in (iii) that $\hat{h}(\omega)$ has a zero of order p at $\omega = \pm\pi$. But $\hat{h}(\omega)$ is also 2π periodic, so (7.73) implies that $\hat{\phi}(\omega) = O(|\omega - 2l\pi|^p)$ in the neighborhood of $\omega = 2l\pi$, for any $l \neq 0$. Hence $\hat{\phi}^{(m)}(2l\pi) = 0$ if $m < p$.

Since $a_{m,l}^k = 0$ and $\phi(2l\pi) = 0$ when $l \neq 0$, it follows from (7.72) that

$$\hat{\phi}(\omega)\, \delta^{(k)}(\omega - 2l\pi) = 0 \quad \text{for } l \neq 0.$$

The only term that remains in the summation (7.71) is $l = 0$ and inserting (7.72) yields

$$\hat{q}_k(\omega) = (i)^k \frac{1}{2\pi} \left(\hat{\phi}(0)\, \delta^{(k)}(\omega) + \sum_{m=0}^{k-1} a_{m,0}^k\, \delta^{(m)}(\omega) \right) \ .$$

The inverse Fourier transform of $\delta^{(m)}(\omega)$ is $(2\pi)^{-1}(-it)^m$ and Theorem 7.2 proves that $\hat{\phi}(0) \neq 0$. Hence the inverse Fourier transform q_k of $\hat{q}_k$ is a polynomial of degree k. ■ ■

The hypothesis (iv) is called the Fix-Strang condition [445]. The polynomials $\{q_k\}_{0\leqslant k<p}$ define a basis of the space of polynomials of degree $p-1$. The Fix-Strang condition thus proves that ψ has p vanishing moments if and only if any polynomial of degree $p-1$ can be written as a linear expansion of $\{\phi(t-n)\}_{n\in\mathbb{Z}}$. The decomposition coefficients of the polynomials q_k do not have a finite energy because polynomials do not have a finite energy.

Size of Support If f has an isolated singularity at t_0 and if t_0 is inside the support of $\psi_{j,n}(t) = 2^{-j/2}\,\psi(2^{-j}t - n)$, then $\langle f, \psi_{j,n}\rangle$ may have a large amplitude. If ψ has a compact support of size K, at each scale 2^j there are K wavelets $\psi_{j,n}$ whose support includes t_0. To minimize the number of high amplitude coefficients we must reduce the support size of ψ. The following theorem relates the support size of h to the support of ϕ and ψ.

Theorem 7.5 (Compact support)**.** *The scaling function ϕ has a compact support if and only if h has a compact support and their support are equal. If the support of h and ϕ is $[N_1, N_2]$ then the support of ψ is $[(N_1 - N_2 + 1)/2\,,\ (N_2 - N_1 + 1)/2]$.*

Proof. If ϕ has a compact support, since

$$h[n] = \frac{1}{\sqrt{2}} \left\langle \phi\left(\frac{t}{2}\right), \phi(t-n) \right\rangle,$$

we derive that h also has a compact support. Conversely, the scaling function satisfies

$$\frac{1}{\sqrt{2}}\,\phi\left(\frac{t}{2}\right) = \sum_{n=-\infty}^{+\infty} h[n]\,\phi(t-n). \tag{7.74}$$

If h has a compact support then one can prove [193] that ϕ has a compact support. The proof is not reproduced here.

To relate the support of ϕ and h, we suppose that $h[n]$ is non-zero for $N_1 \leqslant n \leqslant N_2$ and that ϕ has a compact support $[K_1, K_2]$. The support of $\phi(t/2)$ is $[2K_1, 2K_2]$. The sum at the right of (7.74) is a function whose support is $[N_1 + K_1, N_2 + K_2]$. The equality proves that the support of ϕ is $[K_1, K_2] = [N_1, N_2]$.

Let us recall from (7.68) and (7.67) that

$$\frac{1}{\sqrt{2}}\,\psi\left(\frac{t}{2}\right) = \sum_{n=-\infty}^{+\infty} g[n]\,\phi(t-n) = \sum_{n=-\infty}^{+\infty} (-1)^{1-n}\,h[1-n]\,\phi(t-n).$$

If the supports of ϕ and h are equal to $[N_1, N_2]$, the sum in the right-hand side has a support equal to $[N_1 - N_2 + 1, N_2 - N_1 + 1]$. Hence ψ has a support equal to $[(N_1 - N_2 + 1)/2, (N_2 - N_1 + 1)/2]$. ■ ■

If h has a finite impulse response in $[N_1, N_2]$, Theorem 7.5 proves that ψ has a support of size $N_2 - N_1$ centered at $1/2$. To minimize the size of the support, we must synthesize conjugate mirror filters with as few non-zero coefficients as possible.

Support Versus Moments The support size of a function and the number of vanishing moments are a priori independent. However, we shall see in Theorem 7.7 that the constraints imposed on orthogonal wavelets imply that if ψ has p vanishing moments then its support is at least of size $2p - 1$. Daubechies wavelets are optimal in the sense that they have a minimum size support for a given number of vanishing moments. When choosing a particular wavelet, we thus face a trade-off between the number of vanishing moments and the support size. If f has few isolated singularities and is very regular between singularities, we must choose a wavelet with many vanishing moments to produce a large number of small wavelet coefficients $\langle f, \psi_{j,n} \rangle$. If the density of singularities increases, it might be better to decrease the size of its support at the cost of reducing the number of vanishing moments. Indeed, wavelets that overlap the singularities create high amplitude coefficients.

The multiwavelet construction of Geronimo, Hardin and Massupust [270] offers more design flexibility by introducing several scaling functions and wavelets. Exercise 7.16 gives an example. Better trade-off can be obtained between the multiwavelets supports and their vanishing moments [446]. However, multiwavelet decompositions are implemented with a slightly more complicated filter bank algorithm than a standard orthogonal wavelet transform.

Regularity The regularity of ψ has mostly a cosmetic influence on the error introduced by thresholding or quantizing the wavelet coefficients. When reconstructing a signal from its wavelet coefficients

$$f = \sum_{j=-\infty}^{+\infty} \sum_{n=-\infty}^{+\infty} \langle f, \psi_{j,n} \rangle\, \psi_{j,n},$$

an error ε added to a coefficient $\langle f, \psi_{j,n} \rangle$ will add the wavelet component $\varepsilon\,\psi_{j,n}$ to the reconstructed signal. If ψ is smooth, then $\varepsilon\,\psi_{j,n}$ is a smooth error. For image coding applications, a smooth error is often less visible than an irregular error, even though they have the same energy. Better quality images are obtained with wavelets that are continuously differentiable than with the discontinuous Haar wavelet. The following theorem due to Tchamitchian [454] relates the uniform Lipschitz regularity of ϕ and ψ to the number of zeroes of $\hat{h}(\omega)$ at $\omega = \pi$.

Theorem 7.6 (Tchamitchian)**.** *Let $\hat{h}(\omega)$ be a conjugate mirror filter with p zeroes at π and which satisfies the sufficient conditions of Theorem 7.2. Let us perform the factorization*

$$\hat{h}(\omega) = \sqrt{2}\left(\frac{1+\mathrm{e}^{i\omega}}{2}\right)^p \hat{l}(\omega).$$

If $\sup_{\omega\in\mathbb{R}} |\hat{l}(\omega)| = B$ then ψ and ϕ are uniformly Lipschitz α for

$$\alpha < \alpha_0 = p - \log_2 B - 1. \tag{7.75}$$

Proof. This result is proved by showing that there exist $C_1 > 0$ and $C_2 > 0$ such that for all $\omega \in \mathbb{R}$

$$|\hat{\phi}(\omega)| \leqslant C_1 (1+|\omega|)^{-p+\log_2 B} \tag{7.76}$$
$$|\hat{\psi}(\omega)| \leqslant C_2 (1+|\omega|)^{-p+\log_2 B}. \tag{7.77}$$

The Lipschitz regularity of ϕ and ψ is then derived from Theorem 6.1, which shows that if $\int_{-\infty}^{+\infty}(1+|\omega|^\alpha)\,|\hat{f}(\omega)|\,d\omega < +\infty$, then f is uniformly Lipschitz α.

We proved in (7.32) that $\hat{\phi}(\omega) = \prod_{j=1}^{+\infty} 2^{-1/2}\,\hat{h}(2^{-j}\omega)$. One can verify that

$$\prod_{j=1}^{+\infty} \frac{1+\exp(i2^{-j}\omega)}{2} = \frac{1-\exp(i\omega)}{i\,\omega},$$

hence

$$|\hat{\phi}(\omega)| = \frac{|1-\exp(i\omega)|^p}{|\omega|^p} \prod_{j=1}^{+\infty} |\hat{l}(2^{-j}\omega)|. \tag{7.78}$$

Let us now compute an upper bound for $\prod_{j=1}^{+\infty} |\hat{l}(2^{-j}\omega)|$. At $\omega = 0$ we have $\hat{h}(0) = \sqrt{2}$ so $\hat{l}(0) = 1$. Since $\hat{h}(\omega)$ is continuously differentiable at $\omega = 0$, $\hat{l}(\omega)$ is also continuously differentiable at $\omega = 0$. We thus derive that there exists $\varepsilon > 0$ such that if $|\omega| < \varepsilon$ then $|\hat{l}(\omega)| \leqslant 1 + K|\omega|$. Consequently

$$\sup_{|\omega|\leqslant\varepsilon} \prod_{j=1}^{+\infty} |\hat{l}(2^{-j}\omega)| \leqslant \sup_{|\omega|\leqslant\varepsilon} \prod_{j=1}^{+\infty} (1+K|2^{-j}\omega|) \leqslant \mathrm{e}^{K\varepsilon}. \tag{7.79}$$

If $|\omega| > \varepsilon$, there exists $J \geqslant 1$ such that $2^{J-1}\varepsilon \leqslant |\omega| \leqslant 2^J\varepsilon$ and we decompose

$$\prod_{j=1}^{+\infty} \hat{l}(2^{-j}\omega) = \prod_{j=1}^{J} |\hat{l}(2^{-j}\omega)| \prod_{j=1}^{+\infty} |\hat{l}(2^{-j-J}\omega)|. \tag{7.80}$$

Since $\sup_{\omega\in\mathbb{R}} |\hat{l}(\omega)| = B$, inserting (7.79) yields for $|\omega| > \varepsilon$

$$\prod_{j=1}^{+\infty} \hat{l}(2^{-j}\omega) \leqslant B^J\,\mathrm{e}^{K\varepsilon} = \mathrm{e}^{K\varepsilon}\,2^{J\log_2 B}. \tag{7.81}$$

Since $2^J \leqslant \varepsilon^{-1}2|\omega|$, this proves that

$$\forall \omega \in \mathbb{R} \quad , \quad \prod_{j=1}^{+\infty} \hat{l}(2^{-j}\omega) \leqslant \mathrm{e}^{K\varepsilon}\left(1 + \frac{|2\omega|^{\log_2 B}}{\varepsilon^{\log_2 B}}\right).$$

Equation (7.76) is derived from (7.78) and this last inequality. Since $|\hat{\psi}(2\omega)| = 2^{-1/2}\,|\hat{h}(\omega+\pi)|\,|\hat{\phi}(\omega)|$, (7.77) is obtained from (7.76). ■ ■

This theorem proves that if $B < 2^{p-1}$ then $\alpha_0 > 0$. It means that ϕ and ψ are uniformly continuous. For any $m > 0$, if $B < 2^{p-1-m}$ then $\alpha_0 > m$ so ψ and ϕ are m times continuously differentiable. Theorem 7.4 shows that the number p of zeros of $\hat{h}(\omega)$ at π is equal to the number of vanishing moments of ψ. A priori, we are not guaranteed that increasing p will improve the wavelet regularity, since B might increase as well. However, for important families of conjugate mirror filters such as splines or Daubechies filters, B increases more slowly than p, which implies that wavelet regularity increases with the number of vanishing moments. Let us emphasize that the number of vanishing moments and the regularity of orthogonal wavelets are related but it is the number of vanishing moments and not the regularity that affects the amplitude of the wavelet coefficients at fine scales.

7.2.2 Shannon, Meyer and Battle-Lemarié Wavelets

We study important classes of wavelets whose Fourier transforms are derived from the general formula proved in Theorem 7.3,

$$\hat{\psi}(\omega) = \frac{1}{\sqrt{2}}\,\hat{g}\left(\frac{\omega}{2}\right)\,\hat{\phi}\left(\frac{\omega}{2}\right) = \frac{1}{\sqrt{2}}\,\exp\left(\frac{-i\omega}{2}\right)\,\hat{h}^*\left(\frac{\omega}{2}+\pi\right)\hat{\phi}\left(\frac{\omega}{2}\right). \tag{7.82}$$

Shannon Wavelet The Shannon wavelet is constructed from the Shannon multiresolution approximation, which approximates functions by their restriction to low frequency intervals. It corresponds to $\hat{\phi} = \mathbf{1}_{[-\pi,\pi]}$ and $\hat{h}(\omega) = \sqrt{2}\,\mathbf{1}_{[-\pi/2,\pi/2]}(\omega)$ for $\omega \in [-\pi,\pi]$. We derive from (7.82) that

$$\hat{\psi}(\omega) = \begin{cases} \exp\left(-i\omega/2\right) & \text{if } \omega \in [-2\pi,-\pi]\cup[\pi,2\pi] \\ 0 & \text{otherwise} \end{cases} \tag{7.83}$$

and hence

$$\psi(t) = \frac{\sin 2\pi(t-1/2)}{2\pi(t-1/2)} - \frac{\sin \pi(t-1/2)}{\pi(t-1/2)}.$$

This wavelet is $\mathbf{C}^\infty$ but has a slow asymptotic time decay. Since $\hat{\psi}(\omega)$ is zero in the neighborhood of $\omega = 0$, all its derivatives are zero at $\omega = 0$. Theorem 7.4 thus implies that ψ has an infinite number of vanishing moments.

Since $\hat{\psi}(\omega)$ has a compact support we know that $\psi(t)$ is $\mathbf{C}^\infty$. However $|\psi(t)|$ decays only like $|t|^{-1}$ at infinity because $\hat{\psi}(\omega)$ is discontinuous at $\pm\pi$ and $\pm 2\pi$.

Meyer Wavelets A Meyer wavelet [374] is a frequency band-limited function whose Fourier transform is smooth, unlike the Fourier transform of the Shannon wavelet. This smoothness provides a much faster asymptotic decay in time. These wavelets are constructed with conjugate mirror filters $\hat{h}(\omega)$ that are $\mathbf{C}^n$ and satisfy

$$\hat{h}(\omega) = \begin{cases} \sqrt{2} & \text{if } \omega \in [-\pi/3,\pi/3] \\ 0 & \text{if } \omega \in [-\pi,-2\pi/3]\cup[2\pi/3,\pi] \end{cases}. \tag{7.84}$$

The only degree of freedom is the behavior of $\hat{h}(\omega)$ in the transition bands $[-2\pi/3,-\pi/3]\cup[\pi/3,2\pi/3]$. It must satisfy the quadrature condition

$$|\hat{h}(\omega)|^2 + |\hat{h}(\omega+\pi)|^2 = 2, \tag{7.85}$$

and to obtain $\mathbf{C}^n$ junctions at $|\omega| = \pi/3$ and $|\omega| = 2\pi/3$, the n first derivatives must vanish at these abscissa. One can construct such functions that are $\mathbf{C}^\infty$.

The scaling function $\hat{\phi}(\omega) = \prod_{p=1}^{+\infty} 2^{-1/2}\,\hat{h}(2^{-p}\omega)$ has a compact support and one can verify that

$$\hat{\phi}(\omega) = \begin{cases} 2^{-1/2}\,\hat{h}(\omega/2) & \text{if } |\omega| \leqslant 4\pi/3 \\ 0 & \text{if } |\omega| > 4\pi/3 \end{cases}. \tag{7.86}$$

The resulting wavelet (7.82) is

$$\hat{\psi}(\omega) = \begin{cases} 0 & \text{if } |\omega| \leqslant 2\pi/3 \\ 2^{-1/2}\,\hat{g}(\omega/2) & \text{if } 2\pi/3 \leqslant |\omega| \leqslant 4\pi/3 \\ 2^{-1/2}\,\exp(-i\omega/2)\,\hat{h}(\omega/4) & \text{if } 4\pi/3 \leqslant |\omega| \leqslant 8\pi/3 \\ 0 & \text{if } |\omega| > 8\pi/3 \end{cases}. \tag{7.87}$$

The functions ϕ and ψ are $\mathbf{C}^\infty$ because their Fourier transforms have a compact support. Since $\hat{\psi}(\omega) = 0$ in the neighborhood of $\omega = 0$, all its derivatives are zero at $\omega = 0$, which proves that ψ has an infinite number of vanishing moments.

If $\hat{h}$ is $\mathbf{C}^n$ then $\hat{\psi}$ and $\hat{\phi}$ are also $\mathbf{C}^n$. The discontinuities of the $(n+1)^{th}$ derivative of $\hat{h}$ are generally at the junction of the transition band $|\omega| = \pi/3\,,\,2\pi/3$, in which case one can show that there exists A such that

$$|\phi(t)| \leqslant A\,(1+|t|)^{-n-1} \quad \text{and} \quad |\psi(t)| \leqslant A\,(1+|t|)^{-n-1}\,.$$

Although the asymptotic decay of ψ is fast when n is large, its effective numerical decay may be relatively slow, which is reflected by the fact that A is quite large. As a consequence, a Meyer wavelet transform is generally implemented in the Fourier domain. Section 8.4.2 relates these wavelet bases to lapped orthogonal transforms applied in the Fourier domain. One can prove [18] that there exists no orthogonal wavelet that is $\mathbf{C}^\infty$ and has an exponential decay.

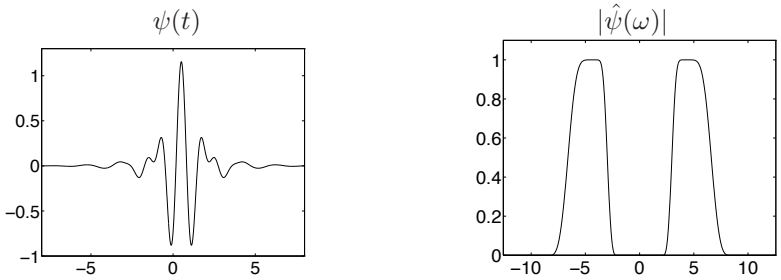

Figure 7.8: Meyer wavelet ψ and its Fourier transform modulus computed with (7.89).

Example 7.10. *To satisfy the quadrature condition (7.85), one can verify that* $\hat{h}$ *in (7.84) may be defined on the transition bands by*

$$\hat{h}(\omega) = \sqrt{2}\,\cos\left[\frac{\pi}{2}\,\beta\left(\frac{3|\omega|}{\pi} - 1\right)\right] \quad \textit{for } |\omega| \in [\pi/3, 2\pi/3]\ ,$$

where $\beta(x)$ *is a function that goes from* 0 *to* 1 *on the interval* $[0,1]$ *and satisfies*

$$\forall x \in [0,1] \quad , \quad \beta(x) + \beta(1-x) = 1. \tag{7.88}$$

An example due to Daubechies [18] is

$$\beta(x) = x^4\,(35 - 84\,x + 70\,x^2 - 20\,x^3). \tag{7.89}$$

The resulting $\hat{h}(\omega)$ *has* $n = 3$ *vanishing derivatives at* $|\omega| = \pi/3\,,\, 2\pi/3$. *Figure 7.8 displays the corresponding wavelet* ψ.

Haar Wavelet The Haar basis is obtained with a multiresolution of piecewise constant functions. The scaling function is $\phi = \mathbf{1}_{[0,1]}$. The filter $h[n]$ given in (7.46) has two non-zero coefficients equal to $2^{-1/2}$ at $n = 0$ and $n = 1$. Hence

$$\frac{1}{\sqrt{2}}\,\psi\left(\frac{t}{2}\right) = \sum_{n=-\infty}^{+\infty} (-1)^{1-n}\,h[1-n]\,\phi(t-n) = \frac{1}{\sqrt{2}}\Big(\phi(t-1) - \phi(t)\Big),$$

so

$$\psi(t) = \begin{cases} -1 & \text{if } 0 \leqslant t < 1/2 \\ 1 & \text{if } 1/2 \leqslant t < 1 \\ 0 & \text{otherwise} \end{cases} \tag{7.90}$$

The Haar wavelet has the shortest support among all orthogonal wavelets. It is not well adapted to approximating smooth functions because it has only one vanishing moment.

Battle-Lemarié Wavelets Polynomial spline wavelets introduced by Battle [97] and Lemarié [344] are computed from spline multiresolution approximations. The expressions of $\hat{\phi}(\omega)$ and $\hat{h}(\omega)$ are given respectively by (7.18) and (7.48). For splines of degree m, $\hat{h}(\omega)$ and its first m derivatives are zero at $\omega = \pi$. Theorem 7.4 derives that ψ has $m+1$ vanishing moments. It follows from (7.82) that

$$\hat{\psi}(\omega) = \frac{\exp(-i\omega/2)}{\omega^{m+1}}\,\sqrt{\frac{S_{2m+2}(\omega/2+\pi)}{S_{2m+2}(\omega)\,S_{2m+2}(\omega/2)}}.$$

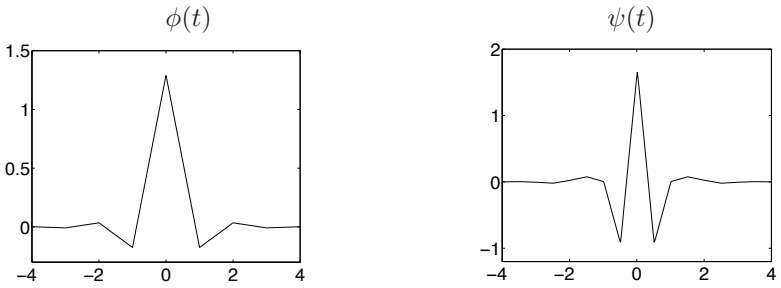

Figure 7.9: Linear spline Battle-Lemarié scaling function ϕ and wavelet ψ.

This wavelet ψ has an exponential decay. Since it is a polynomial spline of degree m, it is $m-1$ times continuously differentiable. Polynomial spline wavelets are less regular than Meyer wavelets but have faster time asymptotic decay. For m odd, ψ is symmetric about $1/2$. For m even it is antisymmetric about $1/2$. Figure 7.5 gives the graph of the cubic spline wavelet ψ corresponding to $m = 3$. For $m = 1$, Figure 7.9 displays linear splines ϕ and ψ. The properties of these wavelets are further studied in [104, 14, 163].

7.2.3 Daubechies Compactly Supported Wavelets

Daubechies wavelets have a support of minimum size for any given number p of vanishing moments. Theorem 7.5 proves that wavelets of compact support are computed with finite impulse response conjugate mirror filters h. We consider real causal filters $h[n]$, which implies that $\hat{h}$ is a trigonometric polynomial:

$$\hat{h}(\omega) = \sum_{n=0}^{N-1} h[n]\, \mathrm{e}^{-in\omega}.$$

To ensure that ψ has p vanishing moments, Theorem 7.4 shows that $\hat{h}$ must have a zero of order p at $\omega = \pi$. To construct a trigonometric polynomial of minimal size, we factor $(1+\mathrm{e}^{-i\omega})^p$, which is a minimum size polynomial having p zeros at $\omega = \pi$:

$$\hat{h}(\omega) = \sqrt{2}\left(\frac{1+\mathrm{e}^{-i\omega}}{2}\right)^p R(\mathrm{e}^{-i\omega}). \tag{7.91}$$

The difficulty is to design a polynomial $R(\mathrm{e}^{-i\omega})$ of minimum degree m such that $\hat{h}$ satisfies

$$|\hat{h}(\omega)|^2 + |\hat{h}(\omega+\pi)|^2 = 2. \tag{7.92}$$

As a result, h has $N = m+p+1$ non-zero coefficients. The following theorem by Daubechies [193] proves that the minimum degree of R is $m = p-1$.

Theorem 7.7 (Daubechies)**.** *A real conjugate mirror filter h, such that $\hat{h}(\omega)$ has p zeroes at $\omega = \pi$, has at least $2p$ non-zero coefficients. Daubechies filters have $2p$ non-zero coefficients.*

Proof. The proof is constructive and computes the Daubechies filters. Since $h[n]$ is real, $|\hat{h}(\omega)|^2$ is an even function and can thus be written as a polynomial in $\cos\omega$. Hence $|R(\mathrm{e}^{-i\omega})|^2$ defined in (7.91) is a polynomial in $\cos\omega$ that we can also write as a polynomial $P(\sin^2(\omega/2))$

$$|\hat{h}(\omega)|^2 = 2\left(\cos\frac{\omega}{2}\right)^{2p} P\left(\sin^2\frac{\omega}{2}\right). \tag{7.93}$$

The quadrature condition (7.92) is equivalent to

$$(1-y)^p\, P(y) + y^p\, P(1-y) = 1, \tag{7.94}$$

for any $y = \sin^2(\omega/2) \in [0,1]$. To minimize the number of non-zero terms of the finite Fourier series $\hat{h}(\omega)$, we must find the solution $P(y) \geqslant 0$ of minimum degree, which is obtained with the Bezout theorem on polynomials.

Theorem 7.8 (Bezout). *Let $Q_1(y)$ and $Q_2(y)$ be two polynomials of degrees n_1 and n_2 with no common zeroes. There exist two unique polynomials $P_1(y)$ and $P_2(y)$ of degrees n_2-1 and n_1-1 such that*

$$P_1(y)\,Q_1(y) + P_2(y)\,Q_2(y) = 1. \tag{7.95}$$

The proof of this classical result is in [18]. Since $Q_1(y) = (1-y)^p$ and $Q_2(y) = y^p$ are two polynomials of degree p with no common zeros, the Bezout theorem proves that there exist two unique polynomials $P_1(y)$ and $P_2(y)$ such that

$$(1-y)^p\,P_1(y) + y^p\,P_2(y) = 1.$$

The reader can verify that $P_2(y) = P_1(1-y) = P(1-y)$ with

$$P(y) = \sum_{k=0}^{p-1} \binom{p-1+k}{k} y^k. \tag{7.96}$$

Clearly $P(y) \geqslant 0$ for $y \in [0,1]$. Hence $P(y)$ is the polynomial of minimum degree satisfying (7.94) with $P(y) \geqslant 0$.

Minimum Phase Factorization Now we need to construct a minimum degree polynomial

$$R(\mathrm{e}^{-i\omega}) = \sum_{k=0}^{m} r_k\,\mathrm{e}^{-ik\omega} = r_0 \prod_{k=0}^{m} (1 - a_k\,\mathrm{e}^{-i\omega})$$

such that $|R(\mathrm{e}^{-i\omega})|^2 = P(\sin^2(\omega/2))$. Since its coefficients are real, $R^*(\mathrm{e}^{-i\omega}) = R(\mathrm{e}^{i\omega})$ and hence

$$|R(\mathrm{e}^{-i\omega})|^2 = R(\mathrm{e}^{-i\omega})\,R(\mathrm{e}^{i\omega}) = P\left(\frac{2 - \mathrm{e}^{i\omega} - \mathrm{e}^{-i\omega}}{4}\right) = Q(\mathrm{e}^{-i\omega}). \tag{7.97}$$

This factorization is solved by extending it to the whole complex plane with the variable $z = \mathrm{e}^{-i\omega}$:

$$R(z)\,R(z^{-1}) = r_0^2 \prod_{k=0}^{m} (1 - a_k\,z)\,(1 - a_k\,z^{-1}) = Q(z) = P\left(\frac{2 - z - z^{-1}}{4}\right). \tag{7.98}$$

Let us compute the roots of $Q(z)$. Since $Q(z)$ has real coefficients if c_k is a root, then c_k^* is also a root and since it is a function of $z + z^{-1}$ if c_k is a root then $1/c_k$ and hence $1/c_k^*$ are also roots. To design $R(z)$ that satisfies (7.98), we choose each root a_k of $R(z)$ among a pair $(c_k, 1/c_k)$ and include a_k^* as a root to obtain real coefficients. This procedure yields a polynomial of minimum degree $m = p-1$, with $r_0^2 = Q(0) = P(1/2) = 2^{p-1}$. The resulting filter h of minimum size has $N = p + m + 1 = 2p$ non-zero coefficients.

Among all possible factorizations, the minimum phase solution $R(\mathrm{e}^{i\omega})$ is obtained by choosing a_k among $(c_k, 1/c_k)$ to be inside the unit circle $|a_k| \leqslant 1$ [50]. The resulting causal filter h has an energy maximally concentrated at small abscissa $n \geqslant 0$. It is a Daubechies filter of order p. ■ ■

The constructive proof of this theorem synthesizes causal conjugate mirror filters of size $2p$. Table 7.2 gives the coefficients of these Daubechies filters for $2 \leqslant p \leqslant 10$. The following theorem derives that Daubechies wavelets calculated with these conjugate mirror filters have a support of minimum size.

Theorem 7.9 (Daubechies). *If ψ is a wavelet with p vanishing moments that generates an orthonormal basis of $\mathbf{L^2}(\mathbb{R})$, then it has a support of size larger than or equal to $2p-1$. A Daubechies wavelet has a minimum size support equal to $[-p+1, p]$. The support of the corresponding scaling function ϕ is $[0, 2p-1]$.*

This theorem is a direct consequence of Theorem 7.7. The support of the wavelet, and that of the scaling function, are calculated with Theorem 7.5. When $p = 1$ we get the Haar wavelet. Figure 7.10 displays the graphs of ϕ and ψ for $p = 2, 3, 4$.

The regularity of ϕ and ψ is the same since $\psi(t)$ is a finite linear combination of the $\phi(2t-n)$. This regularity is however difficult to estimate precisely. Let $B = \sup_{\omega \in \mathbb{R}} |R(\mathrm{e}^{-i\omega})|$ where $R(\mathrm{e}^{-i\omega})$ is the trigonometric polynomial defined in (7.91). Theorem 7.6 proves that ψ is at least uniformly

	n	$h_p[n]$
p = 2	0	.482962913145
	1	.836516303738
	2	.224143868042
	3	−.129409522551
p = 3	0	.332670552950
	1	.806891509311
	2	.459877502118
	3	−.135011020010
	4	−.085441273882
	5	.035226291882
p = 4	0	.230377813309
	1	.714846570553
	2	.630880767930
	3	−.027983769417
	4	−.187034811719
	5	.030841381836
	6	.032883011667
	7	−.010597401785
p = 5	0	.160102397974
	1	.603829269797
	2	.724308528438
	3	.138428145901
	4	−.242294887066
	5	−.032244869585
	6	.077571493840
	7	−.006241490213
	8	−.012580751999
	9	.003335725285
p = 6	0	.111540743350
	1	.494623890398
	2	.751133908021
	3	.315250351709
	4	−.226264693965
	5	−.129766867567
	6	.097501605587
	7	.027522865530
	8	−.031582039317
	9	.000553842201
	10	.004777257511
	11	−.001077301085
p = 7	0	.077852054085
	1	.396539319482
	2	.729132090846
	3	.469782287405
	4	−.143906003929
	5	−.224036184994
	6	.071309219267
	7	.080612609151
	8	−.038029936935
	9	−.016574541631
	10	.012550998556
	11	.000429577973
	12	−.001801640704
	13	.000353713800

	n	$h_p[n]$
p = 8	0	.054415842243
	1	.312871590914
	2	.675630736297
	3	.585354683654
	4	−.015829105256
	5	−.284015542962
	6	.000472484574
	7	.128747426620
	8	−.017369301002
	9	−.04408825393
	10	.013981027917
	11	.008746094047
	12	−.004870352993
	13	−.000391740373
	14	.000675449406
	15	−.000117476784
p = 9	0	.038077947364
	1	.243834674613
	2	.604823123690
	3	.657288078051
	4	.133197385825
	5	−.293273783279
	6	−.096840783223
	7	.148540749338
	8	.030725681479
	9	−.067632829061
	10	.000250947115
	11	.022361662124
	12	−.004723204758
	13	−.004281503682
	14	.001847646883
	15	.000230385764
	16	−.000251963189
	17	.000039347320
p = 10	0	.026670057901
	1	.188176800078
	2	.527201188932
	3	.688459039454
	4	.281172343661
	5	−.249846424327
	6	−.195946274377
	7	.127369340336
	8	.093057364604
	9	−.071394147166
	10	−.029457536822
	11	.033212674059
	12	.003606553567
	13	−.010733175483
	14	.001395351747
	15	.001992405295
	16	−.000685856695
	17	−.000116466855
	18	.000093588670
	19	−.000013264203

Table 7.2: Daubechies filters for wavelets with p vanishing moments.

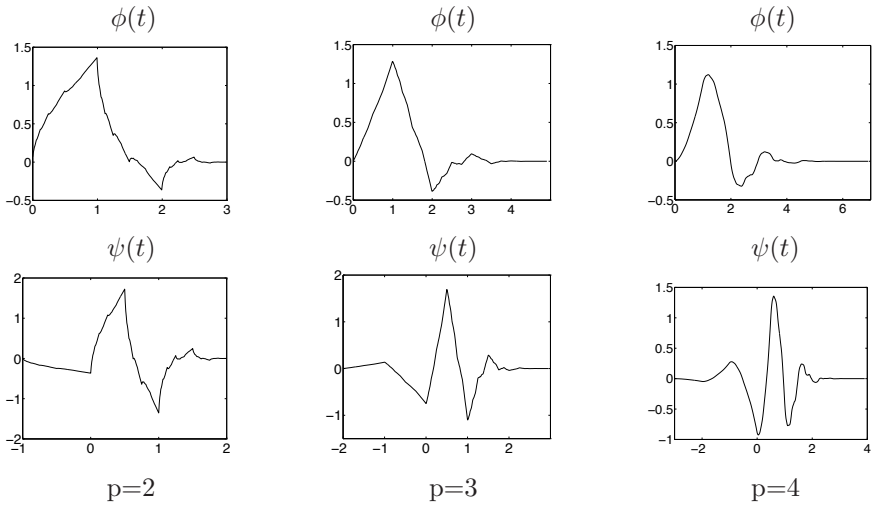

Figure 7.10: Daubechies scaling function ϕ and wavelet ψ with p vanishing moments.

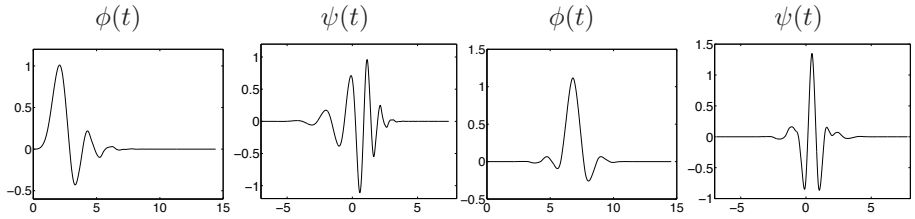

Figure 7.11: Daubechies (first two) and Symmlets (last two) scaling functions and wavelets with $p = 8$ vanishing moments.

Lipschitz α for $\alpha < p - \log_2 B - 1$. For Daubechies wavelets, B increases more slowly than p and Figure 7.10 shows indeed that the regularity of these wavelets increases with p. Daubechies and Lagarias [197] have established a more precise technique that computes the exact Lipschitz regularity of ψ. For $p = 2$ the wavelet ψ is only Lipschitz 0.55 but for $p = 3$ it is Lipschitz 1.08 which means that it is already continuously differentiable. For p large, ϕ and ψ are uniformly Lipschitz α, for α of the order of $0.2\,p$ [167].

Symmlets Daubechies wavelets are very asymmetric because they are constructed by selecting the minimum phase square root of $Q(\mathrm{e}^{-i\omega})$ in (7.97). One can show [50] that filters corresponding to a minimum phase square root have their energy optimally concentrated near the starting point of their support. They are thus highly non-symmetric, which yields very asymmetric wavelets.

To obtain a symmetric or antisymmetric wavelet, the filter h must be symmetric or antisymmetric with respect to the center of its support, which means that $\hat{h}(\omega)$ has a linear complex phase. Daubechies proved [193] that the Haar filter is the only real compactly supported conjugate mirror filter that has a linear phase. The *Symmlet* filters of Daubechies are obtained by optimizing the choice of the square root $R(\mathrm{e}^{-i\omega})$ of $Q(\mathrm{e}^{-i\omega})$ to obtain an almost linear phase. The resulting wavelets still have a minimum support $[-p+1, p]$ with p vanishing moments but they are more symmetric, as illustrated by Figure 7.11 for $p = 8$. The coefficients of the Symmlet filters are in WaveLab. Complex conjugate mirror filters with a compact support and a linear phase can be constructed [351], but they produce complex wavelet coefficients whose real and imaginary parts are redundant when the signal is real.

Coiflets For an application in numerical analysis, Coifman asked Daubechies [193] to construct a family of wavelets ψ that have p vanishing moments and a minimum size support, but whose

scaling functions also satisfy

$$\int_{-\infty}^{+\infty} \phi(t)\,dt = 1 \quad \text{and} \quad \int_{-\infty}^{+\infty} t^k\,\phi(t)\,dt = 0 \quad \text{for } 1 \leqslant k < p. \tag{7.99}$$

Such scaling functions are useful in establishing precise quadrature formulas. If f is $\mathbf{C}^k$ in the neighborhood of $2^J n$ with $k < p$, then a Taylor expansion of f up to order k shows that

$$2^{-J/2}\,\langle f, \phi_{J,n}\rangle \approx f(2^J n) + O(2^{(k+1)J})\ . \tag{7.100}$$

At a fine scale 2^J, the scaling coefficients are thus closely approximated by the signal samples. The order of approximation increases with p. The supplementary condition (7.99) requires increasing the support of ψ; the resulting Coiflet has a support of size $3p-1$ instead of $2p-1$ for a Daubechies wavelet. The corresponding conjugate mirror filters are tabulated in WaveLab.

Audio Filters The first conjugate mirror filters with finite impulse response were constructed in 1986 by Smith and Barnwell [442] in the context of perfect filter bank reconstruction, explained in Section 7.3.2. These filters satisfy the quadrature condition $|\hat{h}(\omega)|^2 + |\hat{h}(\omega+\pi)|^2 = 2$, which is necessary and sufficient for filter bank reconstruction. However, $\hat{h}(0) \neq \sqrt{2}$ so the infinite product of such filters does not yield a wavelet basis of $\mathbf{L^2}(\mathbb{R})$. Instead of imposing any vanishing moments, Smith and Barnwell [442], and later Vaidyanathan and Hoang [470], designed their filters to reduce the size of the transition band, where $|\hat{h}(\omega)|$ decays from nearly $\sqrt{2}$ to nearly 0 in the neighborhood of $\pm\pi/2$. This constraint is important in optimizing the transform code of audio signals, explained in Section 10.3.3. However, many cascades of these filters exhibit wild behavior. The Vaidyanathan-Hoang filters are tabulated in WaveLab. Many other classes of conjugate mirror filters with finite impulse response have been constructed [67, 77]. Recursive conjugate mirror filters may also be designed [299] to minimize the size of the transition band for a given number of zeroes at $\omega = \pi$. These filters have a fast but non-causal recursive implementation for signals of finite size.

7.3 Wavelets and Filter Banks

Decomposition coefficients in a wavelet orthogonal basis are computed with a fast algorithm that cascades discrete convolutions with h and g, and subsamples the output. Section 7.3.1 derives this result from the embedded structure of multiresolution approximations. A direct filter bank analysis is performed in Section 7.3.2, which gives more general perfect reconstruction conditions on the filters. Section 7.3.3 shows that perfect reconstruction filter banks decompose signals in a basis of $\boldsymbol{\ell}^2(\mathbb{Z})$. This basis is orthogonal for conjugate mirror filters.

7.3.1 Fast Orthogonal Wavelet Transform

We describe a fast filter bank algorithm that computes the orthogonal wavelet coefficients of a signal measured at a finite resolution. A fast wavelet transform decomposes successively each approximation $P_{\mathbf{V}_j} f$ into a coarser approximation $P_{\mathbf{V}_{j+1}} f$ plus the wavelet coefficients carried by $P_{\mathbf{W}_{j+1}} f$. In the other direction, the reconstruction from wavelet coefficients recovers each $P_{\mathbf{V}_j} f$ from $P_{\mathbf{V}_{j+1}} f$ and $P_{\mathbf{W}_{j+1}} f$.

Since $\{\phi_{j,n}\}_{n\in\mathbb{Z}}$ and $\{\psi_{j,n}\}_{n\in\mathbb{Z}}$ are orthonormal bases of $\mathbf{V}_j$ and $\mathbf{W}_j$ the projection in these spaces is characterized by

$$a_j[n] = \langle f, \phi_{j,n}\rangle \quad \text{and} \quad d_j[n] = \langle f, \psi_{j,n}\rangle\ .$$

The following theorem [359, 360] shows that these coefficients are calculated with a cascade of discrete convolutions and subsamplings. We denote $\bar{x}[n] = x[-n]$ and

$$\check{x}[n] = \begin{cases} x[p] & \text{if } n = 2p \\ 0 & \text{if } n = 2p+1 \end{cases}\ . \tag{7.101}$$

Theorem 7.10 (Mallat)**.** *At the decomposition*

$$a_{j+1}[p] = \sum_{n=-\infty}^{+\infty} h[n-2p]\, a_j[n] = a_j \star \bar{h}[2p], \tag{7.102}$$

$$d_{j+1}[p] = \sum_{n=-\infty}^{+\infty} g[n-2p]\, a_j[n] = a_j \star \bar{g}[2p]. \tag{7.103}$$

At the reconstruction,

$$\begin{aligned} a_j[p] &= \sum_{n=-\infty}^{+\infty} h[p-2n]\, a_{j+1}[n] + \sum_{n=-\infty}^{+\infty} g[p-2n]\, d_{j+1}[n] \\ &= \check{a}_{j+1} \star h[p] + \check{d}_{j+1} \star g[p]. \end{aligned} \tag{7.104}$$

Proof. Proof of (7.102) Any $\phi_{j+1,p} \in \mathbf{V}_{j+1} \subset \mathbf{V}_j$ can be decomposed in the orthonormal basis $\{\phi_{j,n}\}_{n\in\mathbb{Z}}$ of $\mathbf{V}_j$:

$$\phi_{j+1,p} = \sum_{n=-\infty}^{+\infty} \langle \phi_{j+1,p}, \phi_{j,n} \rangle\, \phi_{j,n}. \tag{7.105}$$

With the change of variable $t' = 2^{-j}t - 2p$ we obtain

$$\begin{aligned} \langle \phi_{j+1,p}, \phi_{j,n} \rangle &= \int_{-\infty}^{+\infty} \frac{1}{\sqrt{2^{j+1}}}\, \phi\Big(\frac{t - 2^{j+1}p}{2^{j+1}}\Big)\, \frac{1}{\sqrt{2^j}}\, \phi^*\Big(\frac{t-2^j n}{2^j}\Big)\, dt \\ &= \int_{-\infty}^{+\infty} \frac{1}{\sqrt{2}}\, \phi\Big(\frac{t}{2}\Big)\, \phi^*(t-n+2p)\, dt \\ &= \Big\langle \frac{1}{\sqrt{2}} \phi\Big(\frac{t}{2}\Big), \phi(t-n+2p) \Big\rangle = h[n-2p]. \end{aligned} \tag{7.106}$$

Hence (7.105) implies that

$$\phi_{j+1,p} = \sum_{n=-\infty}^{+\infty} h[n-2p]\, \phi_{j,n}. \tag{7.107}$$

Computing the inner product of f with the vectors on each side of this equality yields (7.102).

Proof of (7.103) Since $\psi_{j+1,p} \in \mathbf{W}_{j+1} \subset \mathbf{V}_j$, it can be decomposed as

$$\psi_{j+1,p} = \sum_{n=-\infty}^{+\infty} \langle \psi_{j+1,p}, \phi_{j,n} \rangle\, \phi_{j,n}.$$

As in (7.106), the change of variable $t' = 2^{-j}t - 2p$ proves that

$$\langle \psi_{j+1,p}, \phi_{j,n} \rangle = \Big\langle \frac{1}{\sqrt{2}} \psi\left(\frac{t}{2}\right), \phi(t-n+2p) \Big\rangle = g[n-2p] \tag{7.108}$$

and hence

$$\psi_{j+1,p} = \sum_{n=-\infty}^{+\infty} g[n-2p]\, \phi_{j,n}. \tag{7.109}$$

Taking the inner product with f on each side gives (7.103).

Proof of (7.104) Since $\mathbf{W}_{j+1}$ is the orthogonal complement of $\mathbf{V}_{j+1}$ in $\mathbf{V}_j$ the union of the two bases $\{\psi_{j+1,n}\}_{n\in\mathbb{Z}}$ and $\{\phi_{j+1,n}\}_{n\in\mathbb{Z}}$ is an orthonormal basis of $\mathbf{V}_j$. Hence any $\phi_{j,p}$ can be decomposed in this basis:

$$\begin{aligned} \phi_{j,p} &= \sum_{n=-\infty}^{+\infty} \langle \phi_{j,p}, \phi_{j+1,n} \rangle\, \phi_{j+1,n} \\ &\quad + \sum_{n=-\infty}^{+\infty} \langle \phi_{j,p}, \psi_{j+1,n} \rangle\, \psi_{j+1,n}. \end{aligned}$$

Inserting (7.106) and (7.108) yields

$$\phi_{j,p} = \sum_{n=-\infty}^{+\infty} h[p-2n]\,\phi_{j+1,n} + \sum_{n=-\infty}^{+\infty} g[p-2n]\,\psi_{j+1,n}.$$

Taking the inner product with f on both sides of this equality gives (7.104). ■ ■

Theorem 7.10 proves that a_{j+1} and d_{j+1} are computed by taking every other sample of the convolution of a_j with $\bar{h}$ and $\bar{g}$ respectively, as illustrated by Figure 7.12. The filter $\bar{h}$ removes the higher frequencies of the inner product sequence a_j whereas $\bar{g}$ is a high-pass filter which collects the remaining highest frequencies. The reconstruction (7.104) is an interpolation that inserts zeroes to expand a_{j+1} and d_{j+1} and filters these signals, as shown in Figure 7.12.

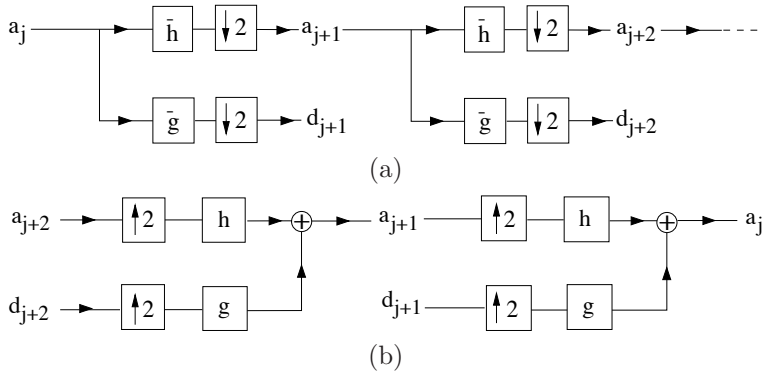

Figure 7.12: (a): A fast wavelet transform is computed with a cascade of filterings with $\bar{h}$ and $\bar{g}$ followed by a factor 2 subsampling. (b): A fast inverse wavelet transform reconstructs progressively each a_j by inserting zeroes between samples of a_{j+1} and d_{j+1}, filtering and adding the output.

An *orthogonal wavelet representation* of $a_L = \langle f, \phi_{L,n}\rangle$ is composed of wavelet coefficients of f at scales $2^L < 2^j \leqslant 2^J$ plus the remaining approximation at the largest scale 2^J:

$$[\{d_j\}_{L<j\leqslant J}\ ,\ a_J]\,. \tag{7.110}$$

It is computed from a_L by iterating (7.102) and (7.103) for $L \leqslant j < J$. Figure 7.7 gives a numerical example computed with the cubic spline filter of Table 7.1. The original signal a_L is recovered from this wavelet representation by iterating the reconstruction (7.104) for $J > j \geqslant L$.

Initialization Most often the discrete input signal $b[n]$ is obtained by a finite resolution device that averages and samples an analog input signal. For example, a CCD camera filters the light intensity by the optics and each photo-receptor averages the input light over its support. A pixel value thus measures average light intensity. If the sampling distance is N^{-1}, to define and compute the wavelet coefficients, we need to associate to $b[n]$ a function $f(t) \in \mathbf{V}_L$ approximated at the scale $2^L = N^{-1}$, and compute $a_L[n] = \langle f, \phi_{L,n}\rangle$. Exercise 7.6 explains how to compute $a_L[n] = \langle f, \phi_{L,n}\rangle$ so that $b[n] = f(N^{-1}n)$.

A simpler and faster approach considers

$$f(t) = \sum_{n=-\infty}^{+\infty} b[n]\,\phi\left(\frac{t-2^L n}{2^L}\right) \in \mathbf{V}_L.$$

Since $\{\phi_{L,n}(t) = 2^{-L/2}\,\phi(2^{-L}t - n)\}_{n\in\mathbb{Z}}$ is orthonormal and $2^L = N^{-1}$,

$$b[n] = N^{1/2}\,\langle f, \phi_{L,n}\rangle = N^{1/2}\,a_L[n]\ .$$

But $\hat{\phi}(0) = \int_{-\infty}^{\infty} \phi(t)\,dt = 1$, so

$$N^{1/2}\,a_L[n] = \int_{-\infty}^{+\infty} f(t)\,\frac{1}{N^{-1}}\,\phi\left(\frac{t-N^{-1}n}{N^{-1}}\right)\,dt$$

is a weighted average of f in the neighborhood of $N^{-1}n$ over a domain proportional to N^{-1}. Hence if f is regular,

$$b[n] = N^{1/2}\, a_L[n] \approx f(N^{-1}n)\ . \tag{7.111}$$

If ψ is a Coiflet and $f(t)$ is regular in the neighborhood of $N^{-1}n$, then (7.100) shows that $N^{-1/2}\, a_L[n]$ is a high order approximation of $f(N^{-1}n)$.

Finite Signals Let us consider a signal f whose support is in $[0,1]$ and which is approximated with a uniform sampling at intervals N^{-1}. The resulting approximation a_L has $N = 2^{-L}$ samples. This is the case in Figure 7.7 with $N = 1024$. Computing the convolutions with $\bar{h}$ and $\bar{g}$ at abscissa close to 0 or close to N requires knowing the values of $a_L[n]$ beyond the boundaries $n = 0$ and $n = N - 1$. These boundary problems may be solved with one of the three approaches described in Section 7.5.

Section 7.5.1 explains the simplest algorithm, which periodizes a_L. The convolutions in Theorem 7.10 are replaced by circular convolutions. This is equivalent to decomposing f in a periodic wavelet basis of $\mathbf{L^2}[0,1]$. This algorithm has the disadvantage of creating large wavelet coefficients at the borders.

If ψ is symmetric or antisymmetric, we can use a folding procedure described in Section 7.5.2, which creates smaller wavelet coefficients at the border. It decomposes f in a folded wavelet basis of $\mathbf{L^2}[0,1]$. However, we mentioned in Section 7.2.3 that Haar is the only symmetric wavelet with a compact support. Higher order spline wavelets have a symmetry but h must be truncated in numerical calculations.

The most efficient boundary treatment is described in Section 7.5.3, but the implementation is more complicated. Boundary wavelets which keep their vanishing moments are designed to avoid creating large amplitude coefficients when f is regular. The fast algorithm is implemented with special boundary filters, and requires the same number of calculations as the two other methods.

Complexity Suppose that h and g have K non-zero coefficients. Let a_L be a signal of size $N = 2^{-L}$. With appropriate boundary calculations, each a_j and d_j has 2^{-j} samples. Equations (7.102) and (7.103) compute a_{j+1} and d_{j+1} from a_j with $2^{-j}K$ additions and multiplications. The wavelet representation (7.110) is therefore calculated with at most $2KN$ additions and multiplications. The reconstruction (7.104) of a_j from a_{j+1} and d_{j+1} is also obtained with $2^{-j}K$ additions and multiplications. The original signal a_L is thus also recovered from the wavelet representation with at most $2KN$ additions and multiplications.

Wavelet Graphs The graphs of ϕ and ψ are computed numerically with the inverse wavelet transform. If $f = \phi$ then $a_0[n] = \delta[n]$ and $d_j[n] = 0$ for all $L < j \leqslant 0$. The inverse wavelet transform computes a_L and (7.111) shows that

$$N^{1/2}\, a_L[n] \approx \phi(N^{-1}n)\ .$$

If ϕ is regular and N is large enough, we recover a precise approximation of the graph of ϕ from a_L.

Similarly, if $f = \psi$ then $a_0[n] = 0$, $d_0[n] = \delta[n]$ and $d_j[n] = 0$ for $L < j < 0$. Then $a_L[n]$ is calculated with the inverse wavelet transform and $N^{1/2}\, a_L[n] \approx \psi(N^{-1}n)$. The Daubechies wavelets and scaling functions in Figure 7.10 are calculated with this procedure.

7.3.2 Perfect Reconstruction Filter Banks

The fast discrete wavelet transform decomposes signals into low-pass and high-pass components subsampled by 2; the inverse transform performs the reconstruction. The study of such classical multirate filter banks became a major signal processing topic in 1976, when Croisier, Esteban and Galand [188] discovered that it is possible to perform such decompositions and reconstructions with *quadrature mirror filters* (Exercise 7.7). However, besides the simple Haar filter, a quadrature mirror filter can not have a finite impulse response. In 1984, Smith and Barnwell [443] and Mintzer [375] found necessary and sufficient conditions for obtaining perfect reconstruction orthogonal filters

with a finite impulse response, that they called *conjugate mirror filters*. The theory was completed by the biorthogonal equations of Vetterli [472, 471] and the general paraunitary matrix theory of Vaidyanathan [469]. We follow this digital signal processing approach which gives a simple understanding of conjugate mirror filter conditions. More complete presentations of filter banks properties can be found in [1, 2, 62, 66, 67].

Filter Bank A two-channel multirate filter bank convolves a signal a_0 with a low-pass filter $\bar{h}[n] = h[-n]$ and a high-pass filter $\bar{g}[n] = g[-n]$ and subsamples by 2 the output:

$$a_1[n] = a_0 \star \bar{h}[2n] \quad \text{and} \quad d_1[n] = a_0 \star \bar{g}[2n]. \tag{7.112}$$

A reconstructed signal $\tilde{a}_0$ is obtained by filtering the zero expanded signals with a dual low-pass filter $\tilde{h}$ and a dual high-pass filter $\tilde{g}$, as shown in Figure 7.13. With the zero insertion notation (7.101) it yields

$$\tilde{a}_0[n] = \check{a}_1 \star \tilde{h}[n] + \check{d}_1 \star \tilde{g}[n]. \tag{7.113}$$

We study necessary and sufficient conditions on h, g, $\tilde{h}$ and $\tilde{g}$ to guarantee a perfect reconstruction $\tilde{a}_0 = a_0$.

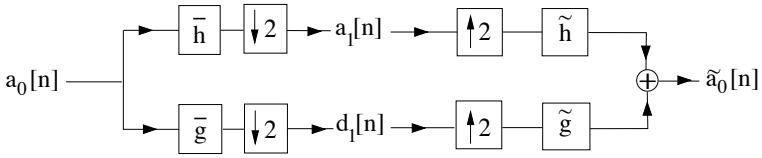

Figure 7.13: The input signal is filtered by a low-pass and a high-pass filter and subsampled. The reconstruction is performed by inserting zeroes and filtering with dual filters $\tilde{h}$ and $\tilde{g}$.

Subsampling and Zero Interpolation Subsamplings and expansions with zero insertions have simple expressions in the Fourier domain. Since $\hat{x}(\omega) = \sum_{n=-\infty}^{+\infty} x[n]\, \mathrm{e}^{-in\omega}$ the Fourier series of the subsampled signal $y[n] = x[2n]$ can be written

$$\hat{y}(2\omega) = \sum_{n=-\infty}^{+\infty} x[2n]\, \mathrm{e}^{-i2n\omega} = \frac{1}{2}\Big(\hat{x}(\omega) + \hat{x}(\omega+\pi)\Big). \tag{7.114}$$

The component $\hat{x}(\omega+\pi)$ creates a frequency folding. This *aliasing* must be canceled at the reconstruction.

The insertion of zeros defines

$$y[n] = \check{x}[n] = \begin{cases} x[p] & \text{if } n = 2p \\ 0 & \text{if } n = 2p+1 \end{cases},$$

whose Fourier transform is

$$\hat{y}(\omega) = \sum_{n=-\infty}^{+\infty} x[n]\, \mathrm{e}^{-i2n\omega} = \hat{x}(2\omega). \tag{7.115}$$

The following theorem gives Vetterli's [471] biorthogonal conditions, which guarantee that $\tilde{a}_0 = a_0$.

Theorem 7.11 (Vetterli)**.** *The filter bank performs an exact reconstruction for any input signal if and only if*

$$\hat{h}^*(\omega+\pi)\, \widehat{\tilde{h}}(\omega) + \hat{g}^*(\omega+\pi)\, \widehat{\tilde{g}}(\omega) = 0, \tag{7.116}$$

and

$$\hat{h}^*(\omega)\, \widehat{\tilde{h}}(\omega) + \hat{g}^*(\omega)\, \widehat{\tilde{g}}(\omega) = 2. \tag{7.117}$$

Proof. We first relate the Fourier transform of a_1 and d_1 to the Fourier transform of a_0. Since h and g are real, the transfer functions of $\bar{h}$ and $\bar{g}$ are respectively $\hat{h}(-\omega) = \hat{h}^*(\omega)$ and $\hat{g}(-\omega) = \hat{g}^*(\omega)$. By using (7.114), we derive from the definition (7.112) of a_1 and d_1 that

$$\hat{a}_1(2\omega) = \frac{1}{2}\left(\hat{a}_0(\omega)\,\hat{h}^*(\omega) + \hat{a}_0(\omega+\pi)\,\hat{h}^*(\omega+\pi)\right), \tag{7.118}$$

$$\hat{d}_1(2\omega) = \frac{1}{2}\left(\hat{a}_0(\omega)\,\hat{g}^*(\omega) + \hat{a}_0(\omega+\pi)\,\hat{g}^*(\omega+\pi)\right). \tag{7.119}$$

The expression (7.113) of $\tilde{a}_0$ and the zero insertion property (7.115) also imply

$$\widehat{\tilde{a}}_0(\omega) = \hat{a}_1(2\omega)\,\widehat{\tilde{h}}(\omega) + \hat{d}_1(2\omega)\,\widehat{\tilde{g}}(\omega). \tag{7.120}$$

Hence

$$\begin{aligned}\widehat{\tilde{a}}_0(\omega) = {} & \frac{1}{2}\left(\hat{h}^*(\omega)\,\widehat{\tilde{h}}(\omega) + \hat{g}^*(\omega)\,\widehat{\tilde{g}}(\omega)\right)\hat{a}_0(\omega) + \\ & \frac{1}{2}\left(\hat{h}^*(\omega+\pi)\,\widehat{\tilde{h}}(\omega) + \hat{g}^*(\omega+\pi)\,\widehat{\tilde{g}}(\omega)\right)\hat{a}_0(\omega+\pi).\end{aligned}$$

To obtain $a_0 = \tilde{a}_0$ for all a_0, the filters must cancel the aliasing term $\hat{a}_0(\omega+\pi)$ and guarantee a unit gain for $\hat{a}_0(\omega)$, which proves equations (7.116) and (7.117). ■ ■

Theorem 7.11 proves that the reconstruction filters $\tilde{h}$ and $\tilde{g}$ are entirely specified by the decomposition filters h and g. In matrix form, it can be rewritten

$$\begin{pmatrix} \hat{h}(\omega) & \hat{g}(\omega) \\ \hat{h}(\omega+\pi) & \hat{g}(\omega+\pi) \end{pmatrix} \times \begin{pmatrix} \widehat{\tilde{h}}^*(\omega) \\ \widehat{\tilde{g}}^*(\omega) \end{pmatrix} = \begin{pmatrix} 2 \\ 0 \end{pmatrix}. \tag{7.121}$$

The inversion of this 2×2 matrix yields

$$\begin{pmatrix} \widehat{\tilde{h}}^*(\omega) \\ \widehat{\tilde{g}}^*(\omega) \end{pmatrix} = \frac{2}{\Delta(\omega)} \begin{pmatrix} \hat{g}(\omega+\pi) \\ -\hat{h}(\omega+\pi) \end{pmatrix} \tag{7.122}$$

where $\Delta(\omega)$ is the determinant

$$\Delta(\omega) = \hat{h}(\omega)\,\hat{g}(\omega+\pi) - \hat{h}(\omega+\pi)\,\hat{g}(\omega). \tag{7.123}$$

The reconstruction filters are stable only if the determinant does not vanish for all $\omega \in [-\pi, \pi]$. Vaidyanathan [469] has extended this result to multirate filter banks with an arbitrary number M of channels by showing that the resulting matrices of filters satisfy paraunitary properties [66].

Finite Impulse Response When all filters have a finite impulse response, the determinant $\Delta(\omega)$ can be evaluated. This yields simpler relations between the decomposition and reconstruction filters.

Theorem 7.12. *Perfect reconstruction filters satisfy*

$$\hat{h}^*(\omega)\,\widehat{\tilde{h}}(\omega) + \hat{h}^*(\omega+\pi)\,\widehat{\tilde{h}}(\omega+\pi) = 2. \tag{7.124}$$

For finite impulse response filters, there exist $a \in \mathbb{R}$ and $l \in \mathbb{Z}$ such that

$$\hat{g}(\omega) = a\,\mathrm{e}^{-i(2l+1)\omega}\,\widehat{\tilde{h}}^*(\omega+\pi) \quad \text{and} \quad \widehat{\tilde{g}}(\omega) = a^{-1}\,\mathrm{e}^{-i(2l+1)\omega}\,\hat{h}^*(\omega+\pi). \tag{7.125}$$

Proof. Equation (7.122) proves that

$$\widehat{\tilde{h}}^*(\omega) = \frac{2}{\Delta(\omega)}\,\hat{g}(\omega+\pi) \quad \text{and} \quad \widehat{\tilde{g}}^*(\omega) = \frac{-2}{\Delta(\omega)}\,\hat{h}(\omega+\pi). \tag{7.126}$$

Hence

$$\hat{g}(\omega)\,\widehat{\tilde{g}}^*(\omega) = -\frac{\Delta(\omega+\pi)}{\Delta(\omega)}\,\widehat{\tilde{h}}^*(\omega+\pi)\,\hat{h}(\omega+\pi). \tag{7.127}$$

The definition (7.123) implies that $\Delta(\omega+\pi) = -\Delta(\omega)$. Inserting (7.127) in (7.117) yields (7.124).

The Fourier transform of finite impulse response filters is a finite series in $\exp(\pm in\omega)$. The determinant $\Delta(\omega)$ defined by (7.123) is therefore a finite series. Moreover (7.126) proves that $\Delta^{-1}(\omega)$ must also be a finite series. A finite series in $\exp(\pm in\omega)$ whose inverse is also a finite series must have a single term. Since $\Delta(\omega) = -\Delta(\omega+\pi)$ the exponent n must be odd. This proves that there exist $l \in \mathbb{Z}$ and $a \in \mathbb{R}$ such that

$$\Delta(\omega) = -2\,a\,\exp[i(2l+1)\omega]. \tag{7.128}$$

Inserting this expression in (7.126) yields (7.125). ■ ■

The factor a is a gain which is inverse for the decomposition and reconstruction filters and l is a reverse shift. We generally set $a = 1$ and $l = 0$. In the time domain (7.125) can then be rewritten

$$g[n] = (-1)^{1-n}\,\tilde{h}[1-n] \quad \text{and} \quad \tilde{g}[n] = (-1)^{1-n}\,h[1-n]. \tag{7.129}$$

The two pairs of filters (h, g) and $(\tilde{h}, \tilde{g})$ play a symmetric role and can be inverted.

Conjugate Mirror Filters If we impose that the decomposition filter h is equal to the reconstruction filter $\tilde{h}$, then (7.124) is the condition of Smith and Barnwell [443] and Mintzer [375] that defines conjugate mirror filters:

$$|\hat{h}(\omega)|^2 + |\hat{h}(\omega+\pi)|^2 = 2. \tag{7.130}$$

It is identical to the filter condition (7.29) that is required in order to synthesize orthogonal wavelets. The next section proves that it is also equivalent to discrete orthogonality properties.

7.3.3 Biorthogonal Bases of $\ell^2(\mathbb{Z})$

The decomposition of a discrete signal in a multirate filter bank is interpreted as an expansion in a basis of $\ell^2(\mathbb{Z})$. Observe first that the low-pass and high-pass signals of a filter bank computed with (7.112) can be rewritten as inner products in $\ell^2(\mathbb{Z})$:

$$a_1[l] = \sum_{n=-\infty}^{+\infty} a_0[n]\,h[n-2l] = \langle a_0[n], h[n-2l]\rangle, \tag{7.131}$$

$$d_1[l] = \sum_{n=-\infty}^{+\infty} a_0[n]\,g[n-2l] = \langle a_0[n], g[n-2l]\rangle. \tag{7.132}$$

The signal recovered by the reconstructing filters is

$$a_0[n] = \sum_{l=-\infty}^{+\infty} a_1[l]\,\tilde{h}[n-2l] + \sum_{l=-\infty}^{+\infty} d_1[l]\,\tilde{g}[n-2l]. \tag{7.133}$$

Inserting (7.131) and (7.132) yields

$$a_0[n] = \sum_{l=-\infty}^{+\infty} \langle f[k], h[k-2l]\rangle\,\tilde{h}[n-2l] + \sum_{l=-\infty}^{+\infty} \langle f[k], g[k-2l]\rangle\,\tilde{g}[n-2l]. \tag{7.134}$$

We recognize the decomposition of a_0 over dual families of vectors $\{\tilde{h}[n-2l], \tilde{g}[n-2l]\}_{l\in\mathbb{Z}}$ and $\{h[n-2l], g[n-2l]\}_{l\in\mathbb{Z}}$. The following theorem proves that these two families are biorthogonal.

Theorem 7.13. *If h, g, $\tilde{h}$ and $\tilde{g}$ are perfect reconstruction filters whose Fourier transform is bounded then $\{\tilde{h}[n-2l], \tilde{g}[n-2l]\}_{l\in\mathbb{Z}}$ and $\{h[n-2l], g[n-2l]\}_{l\in\mathbb{Z}}$ are biorthogonal Riesz bases of $\ell^2(\mathbb{Z})$.*

Proof. To prove that these families are biorthogonal we must show that for all $n \in \mathbb{Z}$

$$\langle \tilde{h}[n], h[n-2l]\rangle = \delta[l] \tag{7.135}$$

$$\langle \tilde{g}[n], g[n-2l]\rangle = \delta[l] \tag{7.136}$$

and

$$\langle \tilde{h}[n], g[n-2l] \rangle = \langle \tilde{g}[n], h[n-2l] \rangle = 0. \tag{7.137}$$

For perfect reconstruction filters, (7.124) proves that

$$\frac{1}{2}\left(\hat{h}^*(\omega)\,\widehat{\tilde{h}}(\omega) + \hat{h}^*(\omega+\pi)\,\widehat{\tilde{h}}(\omega+\pi)\right) = 1.$$

In the time domain, this equation becomes

$$\bar{h} \star \tilde{h}[2l] = \sum_{k=-\infty}^{+\infty} \tilde{h}[n]\,\bar{h}[n-2l] = \delta[l], \tag{7.138}$$

which verifies (7.135). The same proof as for (7.124) shows that

$$\frac{1}{2}\left(\hat{g}^*(\omega)\,\widehat{\tilde{g}}(\omega) + \hat{g}^*(\omega+\pi)\,\widehat{\tilde{g}}(\omega+\pi)\right) = 1.$$

In the time domain, this equation yields (7.136). It also follows from (7.122) that

$$\frac{1}{2}\left(\hat{g}^*(\omega)\,\widehat{\tilde{h}}(\omega) + \hat{g}^*(\omega+\pi)\,\widehat{\tilde{h}}(\omega+\pi)\right) = 0,$$

and

$$\frac{1}{2}\left(\hat{h}^*(\omega)\,\widehat{\tilde{g}}(\omega) + \hat{h}^*(\omega+\pi)\,\widehat{\tilde{g}}(\omega+\pi)\right) = 0.$$

The inverse Fourier transforms of these two equations yield (7.137).

To finish the proof, one must show the existence of Riesz bounds. The reader can verify that this is a consequence of the fact that the Fourier transform of each filter is bounded. ■ ■

Orthogonal Bases A Riesz basis is orthonormal if the dual basis is the same as the original basis. For filter banks, this means that $h = \tilde{h}$ and $g = \tilde{g}$. The filter h is then a conjugate mirror filter

$$|\hat{h}(\omega)|^2 + |\hat{h}(\omega+\pi)|^2 = 2. \tag{7.139}$$

The resulting family $\{h[n-2l], g[n-2l]\}_{l\in\mathbb{Z}}$ is an orthogonal basis of $\boldsymbol{\ell}^2(\mathbb{Z})$.

Discrete Wavelet Bases The construction of conjugate mirror filters is simpler than the construction of orthogonal wavelet bases of $\mathbf{L^2}(\mathbb{R})$. Why then should we bother with continuous time models of wavelets, since in any case all computations are discrete and rely on conjugate mirror filters? The reason is that conjugate mirror filters are most often used in filter banks that cascade several levels of filterings and subsamplings. It is thus necessary to understand the behavior of such a cascade [406]. In a wavelet filter bank tree, the output of the low-pass filter $\bar{h}$ is sub-decomposed whereas the output of the high-pass filter $\bar{g}$ is not; this is illustrated in Figure 7.12. Suppose that the sampling distance of the original discrete signal is N^{-1}. We denote $a_L[n]$ this discrete signal, with $2^L = N^{-1}$. At the depth $j - L \geqslant 0$ of this filter bank tree, the low-pass signal a_j and high-pass signal d_j can be written

$$a_j[l] = a_L \star \bar{\phi}_j[2^{j-L}l] = \langle a_L[n], \phi_j[n - 2^{j-L}l] \rangle$$

and

$$d_j[l] = a_L \star \bar{\psi}_j[2^{j-L}l] = \langle a_L[n], \psi_j[n - 2^{j-L}l] \rangle.$$

The Fourier transforms of these equivalent filters are

$$\hat{\phi}_j(\omega) = \prod_{p=0}^{j-L-1} \hat{h}(2^p\omega) \quad \text{and} \quad \hat{\psi}_j(\omega) = \hat{g}(2^{j-L-1}\omega) \prod_{p=0}^{j-L-2} \hat{h}(2^p\omega). \tag{7.140}$$

A filter bank tree of depth $J - L \geqslant 0$, decomposes a_L over the family of vectors

$$\left[\left\{\phi_J[n - 2^{J-L}l]\right\}_{l\in\mathbb{Z}},\ \left\{\psi_j[n - 2^{j-L}l]\right\}_{L<j\leqslant J\,,\,l\in\mathbb{Z}}\right]. \tag{7.141}$$

For conjugate mirror filters, one can verify that this family is an orthonormal basis of $\ell^2(\mathbb{Z})$. These discrete vectors are close to a uniform sampling of the continuous time scaling functions $\phi_j(t) = 2^{-j/2}\phi(2^{-j}t)$ and wavelets $\psi_j(t) = 2^{-j/2}\phi(2^{-j}t)$. When the number $L-j$ of successive convolutions increases, one can verify that $\phi_j[n]$ and $\psi_j[n]$ converge respectively to $N^{-1/2}\,\phi_j(N^{-1}n)$ and $N^{-1/2}\,\psi_j(N^{-1}n)$. The factor $N^{-1/2}$ normalizes the $\ell^2(\mathbb{Z})$ norm of these sampled functions. If $L-j=4$ then $\phi_j[n]$ and $\psi_j[n]$ are already very close to these limit values. The impulse responses $\phi_j[n]$ and $\psi_j[n]$ of the filter bank are thus much closer to continuous time scaling functions and wavelets than they are to the original conjugate mirror filters h and g. This explains why wavelets provide appropriate models for understanding the applications of these filter banks. Chapter 8 relates more general filter banks to wavelet packet bases.

If the decomposition and reconstruction filters of the filter bank are different, the resulting basis (7.141) is non-orthogonal. The stability of this discrete wavelet basis does not degrade when the depth $J-L$ of the filter bank increases. The next section shows that the corresponding continuous time wavelet $\psi(t)$ generates a Riesz basis of $\mathbf{L^2}(\mathbb{R})$.

7.4 Biorthogonal Wavelet Bases

The stability and completeness properties of biorthogonal wavelet bases are described for perfect reconstruction filters h and $\tilde{h}$ having a finite impulse response. The design of linear phase wavelets with compact support is explained in Section 7.4.2.

7.4.1 Construction of Biorthogonal Wavelet Bases

An infinite cascade of perfect reconstruction filters (h, g) and $(\tilde{h}, \tilde{g})$ yields two scaling functions and wavelets whose Fourier transforms satisfy

$$\hat{\phi}(2\omega) = \frac{1}{\sqrt{2}}\,\hat{h}(\omega)\,\hat{\phi}(\omega) \quad , \quad \widehat{\tilde{\phi}}(2\omega) = \frac{1}{\sqrt{2}}\,\widehat{\tilde{h}}(\omega)\,\widehat{\tilde{\phi}}(\omega)\;, \tag{7.142}$$

$$\hat{\psi}(2\omega) = \frac{1}{\sqrt{2}}\,\hat{g}(\omega)\,\hat{\phi}(\omega) \quad , \quad \widehat{\tilde{\psi}}(2\omega) = \frac{1}{\sqrt{2}}\,\widehat{\tilde{g}}(\omega)\,\widehat{\tilde{\phi}}(\omega)\;. \tag{7.143}$$

In the time domain, these relations become

$$\phi(t) = \sqrt{2}\sum_{n=-\infty}^{+\infty} h[n]\,\phi(2t-n) \quad , \quad \tilde{\phi}(t) = \sqrt{2}\sum_{n=-\infty}^{+\infty} \tilde{h}[n]\,\tilde{\phi}(2t-n) \tag{7.144}$$

$$\psi(t) = \sqrt{2}\sum_{n=-\infty}^{+\infty} g[n]\,\phi(2t-n)\;,\; \tilde{\psi}(t) = \sqrt{2}\sum_{n=-\infty}^{+\infty} \tilde{g}[n]\,\tilde{\phi}(2t-n)\;. \tag{7.145}$$

The perfect reconstruction conditions are given by Theorem 7.12. If we normalize the gain and shift to $a=1$ and $l=0$, the filters must satisfy

$$\hat{h}^*(\omega)\,\widehat{\tilde{h}}(\omega) + \hat{h}^*(\omega+\pi)\,\widehat{\tilde{h}}(\omega+\pi) = 2, \tag{7.146}$$

and

$$\hat{g}(\omega) = \mathrm{e}^{-i\omega}\,\widehat{\tilde{h}}^*(\omega+\pi) \quad , \quad \widehat{\tilde{g}}(\omega) = \mathrm{e}^{-i\omega}\,\hat{h}^*(\omega+\pi). \tag{7.147}$$

Wavelets should have a zero average, which means that $\hat{\psi}(0) = \widehat{\tilde{\psi}}(0) = 0$. This is obtained by setting $\hat{g}(0) = \widehat{\tilde{g}}(0) = 0$ and hence $\hat{h}(\pi) = \widehat{\tilde{h}}(\pi) = 0$. The perfect reconstruction condition (7.146) implies that $\hat{h}^*(0)\,\widehat{\tilde{h}}(0) = 2$. Since both filters are defined up to multiplicative constants respectively equal to λ and λ^{-1}, we adjust λ so that $\hat{h}(0) = \widehat{\tilde{h}}(0) = \sqrt{2}$.

In the following, we also suppose that h and $\tilde{h}$ are finite impulse response filters. One can then prove [18] that

$$\hat{\phi}(\omega) = \prod_{p=1}^{+\infty} \frac{\hat{h}(2^{-p}\omega)}{\sqrt{2}} \quad \text{and} \quad \widehat{\tilde{\phi}}(\omega) = \prod_{p=1}^{+\infty} \frac{\widehat{\tilde{h}}(2^{-p}\omega)}{\sqrt{2}} \tag{7.148}$$